

LEARNING TO GROW ARTIFICIAL HIPPOCAMPI IN VISION TRANSFORMERS FOR RESILIENT LIFELONG LEARNING

Chinmay Savadikar*
csavadi@ncsu.edu

Michelle Dai†
mdai@princeton.edu

Tianfu Wu*
tianfu.wu@ncsu.edu

ABSTRACT

Lifelong learning without catastrophic forgetting (i.e., resiliency) possessed by human intelligence is entangled with sophisticated memory mechanisms in the brain, especially the long-term memory (LM) maintained by Hippocampi. To a certain extent, Transformers have emerged as the counterpart “Brain” of Artificial Intelligence (AI), and yet leave the LM component under-explored for lifelong learning settings. This paper presents a method of learning to grow Artificial Hippocampi (ArtiHippo) in Vision Transformers (ViTs) for resilient lifelong learning. With a comprehensive ablation study, the final linear projection layer in the multi-head self-attention (MHSA) block is selected in realizing and growing ArtiHippo. ArtiHippo is represented by a mixture of experts (MoEs). Each expert component is an on-site variant of the linear projection layer, which is maintained via neural architecture search (NAS) with the search space defined by four basic growing operations – skip, reuse, adapt, and new in lifelong learning. The LM of a task consists of two parts: the dedicated expert components (as model parameters) at different layers of a ViT learned via NAS, and the mean class-tokens (as stored latent vectors for measuring task similarity) associated with the expert components. For a new task, a hierarchical task-similarity-oriented exploration-exploitation sampling based NAS is proposed to learn the expert components. The task similarity is measured based on the normalized cosine similarity between the mean class-token of the new task and those of old tasks. The proposed method is complementary to prompt-based lifelong learning with ViTs. In experiments, the proposed method is tested on the challenging Visual Domain Decathlon (VDD) benchmark and the recently proposed 5-Dataset benchmark. It obtains consistently better performance than the prior art with sensible ArtiHippo learned continually.

1 INTRODUCTION

Developing lifelong learning machines is one of the hallmarks of AI, to mimic human intelligence in terms of learning-to-learn to be adaptive and skilled at streaming tasks, or even to emulate human intelligence in some application domains. However, state-of-the-art machine (deep) learning systems realized by Deep Neural Networks (DNNs) have yet to be intelligent in the biological sense from the perspective of lifelong learning, especially plagued with the critical issue known as *catastrophic forgetting* at streaming tasks in a dynamic environment (McCloskey & Cohen, 1989; Thrun & Mitchell, 1995). Catastrophic forgetting simply means that these systems “forget” how to solve old tasks after sequentially and continually trained on a new task using the data of the new task only. Addressing catastrophic forgetting in lifelong learning is a pressing need with potential paradigm-shift impacts in the next wave of trustworthy and/or brain-inspired AI.

To address catastrophic forgetting, one direct methodology is to utilize exemplar-based settings in which a small number of selected training samples stored for each previous task is used in conjunction with the data of a new task in training the model for the new task. Those exemplar-based methods are also referred as *Experience Replay* based methods (Aljundi et al., 2019b; Hayes et al., 2019; Wu et al., 2019). How the exemplars are selected and how they are incorporated in learning a new task distinguish different exemplar-based methods. Although shown as an effective strategy, retaining raw data samples may induce issues on data security and privacy, as well as the long-run sustainability.

To develop exemplar-free methods, three main strategies have been studied in the literature. The first is to regularize the change in model parameters when trained on a new task as done in (Kirkpatrick et al., 2017). The second is to adapt the structure of a network (with the parameters) for the new task from the network learned for the previous tasks, as done in the learn-to-grow (L2G) method (Li et al., 2019) which uses differentiable Neural Architecture Search (NAS)

* Department of Electrical and Computer Engineering, North Carolina State University

† Operations Research & Financial Engineering, Princeton University

to find whether to *reuse*, *adapt* or *new* each layer of a Multi-Layer Percetpron (MLP) or a convolutional neural network (CNN). More recently, with the availability of powerful pretrained Transformers (Vaswani et al., 2017) based Large Foundation Models (LFMs) (Bommasani et al., 2021) (such as the CLIP models (Radford et al., 2021)), the third is to freeze pretrained LFMs and then to learn prompts (or task tokens) instead for lifelong learning, e.g., the learn-to-prompt (L2P) methods (Wang et al., 2022c;b;a; Douillard et al., 2022).

In this paper, we are interested in studying exemplar-free resilient lifelong learning with Vision Transformers (ViTs) (Dosovitskiy et al., 2021). Our goal is to seek alternative formulations that are not built on completely frozen pretrained Transformer models, but can induce plastic and reconfigurable structures for streaming tasks. We are motivated by some fantastic observations of natural intelligence possessed by biological systems (e.g., the human brain) which exhibit remarkable capacity of learning and adapting their structure and function for tackling different tasks throughout their lifespan, while retaining the stability of their core functions. It has been observed in neuroscience that learning and memory are entangled together in a highly sophisticated way (Christophel et al., 2017; Voito & Mrcic-Flogel, 2022). For lifelong learning, the long-term memory (LM) maintained by the hippocampal system plays an important role. A question naturally arises: **What would be the counterpart, Artificial Hippocampi (ArtiHippo), in ViTs to facilitate resilient lifelong learning?**

The L2P methods exploit external LM memory to store the learned task prompts/tokens while using frozen Transformer backbones, which may lack the plasticity needed in resilient lifelong learning, increases the cost (due to the quadratic complexity of Transformer models with respect to the number of tokens), and unnecessarily enforces all tasks encountered in lifelong learning (regardless of their underlying difficulty levels) to use the same frozen network. In this paper, **we seek more integrative memory mechanisms that introduce learnable parts into Transformers (in contrast to be entirely frozen) to induce reconfigurability, selectivity and plasticity in lifelong learning.** To that end, we adapt the learn-to-grow method (Li et al., 2019), but do not apply the NAS with respect to the four operations uniformly across layers in a ViT. Instead, we aim to find the ArtiHippo inside the ViT. As illustrated in Figure 1, the final projection layer in the multi-head self-attention (MHSA) block of a ViT is identified and selected as the ArtiHippo (Sec. 3.1). The learn-to-grow NAS is only applied in maintaining ArtiHippo layers, while other components are frozen to maintain the stability of core functions, as illustrated in Figure 2. Rather than adopting the DARTS (Liu et al., 2019a) NAS used in (Li et al., 2019), the learn-to-grow NAS in this paper is built on the single-path one-shot (SPOS) NAS (Guo et al., 2020), in which we propose a hierarchical exploration-exploitation sampling (Figure 3) strategy for lifelong learning (Sec. 3.2).

In experiments, this paper considers lifelong learning with task indices available in both training and inference, which is often referred to as *task-incremental setup*. When different tasks consist of data from different domains such as the Visual Domain Decathlon (VDD) benchmark (Rebuffi et al., 2017a), it is also related to domain-incremental setup, but without assuming the same output space between tasks, e.g., the same number of classes in classification in different domains. The right of Figure 1 illustrates an example of learned ArtiHippo. With the task indices, the execution of the computational graph for a given task is straightforward. The proposed method achieves zero-forgetting on old tasks. We show the potential of applying our proposed method for class-incremental lifelong learning settings, especially when integrated with the complementary L2P methods.

2 RELATED WORK AND OUR CONTRIBUTIONS

The catastrophic forgetting problem in neural networks (McCloskey & Cohen, 1989) refers to an exponential loss in performance on previous tasks as the network is trained on data from new tasks. Continual learning (Thrun & Mitchell, 1995) aims to solve this problem by enabling the network to perform well on previous tasks when new tasks are introduced. The most straightforward approach to the problem is to retain some exemplars from the previous tasks and replay them to the model along with the data from the current task, referred to as *Experience Replay Based*

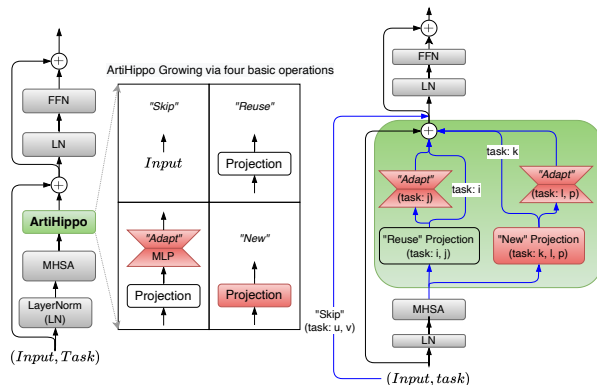


Figure 1: Illustration of the proposed method for task-incremental lifelong learning without any catastrophic forgetting. *Left*: The Multi-Head Self-Attention (MHSA) block in Vision Transformers (Dosovitskiy et al., 2021) with the proposed Artificial Hippocampi (ArtiHippo) replacing the original linear projection layer. *Middle*: The ArtiHippo growing is maintained by four operations, similar in spirit to the learn-to-grow method (Li et al., 2019). *Right*: The ArtiHippo is represented by a mixture of experts with an example for different tasks (e.g., j) started from the task i . See text for details.

approaches (Aljundi et al., 2019b;a; Balaji et al., 2020; Bang et al., 2021; Chaudhry et al., 2021; 2019a; De Lange & Tuytelaars, 2021; Hayes et al., 2020; Lopez-Paz & Ranzato, 2017; Prabhu et al., 2020; Rebuffi et al., 2017b; Chaudhry et al., 2019b; Hayes et al., 2019; Buzzega et al., 2020; Wu et al., 2019; Pham et al., 2021; Cha et al., 2021). Instead of storing raw exemplars, *Generative replay methods* (Shin et al., 2017; Cong et al., 2020) learn the generative process for the data of a task, and replay exemplars sampled from that process along with the data from the current task. For exemplar-free continual learning, *Regularization Based approaches* explicitly control the plasticity of the model by preventing the parameters of the model from deviating too far from their stable values learned on the previous tasks when learning the current task (Aljundi et al., 2018; 2019c; Douillard et al., 2020; Nguyen et al., 2018; Kirkpatrick et al., 2017; Li & Hoiem, 2018; Zenke et al., 2017; Schwarz et al., 2018). These approaches are similar in principle: they aim to balance the stability and plasticity of a fixed-capacity model.

To overcome this constraint, *Dynamic Models* aim to use different parameters per task to avoid use of stored exemplars. Dynamically Expandable Network (Yoon et al., 2018) adds neurons to a network based on learned sparsity constraints and heuristic loss thresholds. PathNet (Fernando et al., 2017) finds task-specific submodules from a dense network, and only trains submodules not used by other tasks. Progressive Neural Networks (Rusu et al., 2016) learn a new network per task and adds lateral connections to the previous tasks’ networks. (Rebuffi et al., 2017a) learns residual adapters which are added between the convolutional and batch normalization layers. (Aljundi et al., 2017) learns an expert network per task by transferring the expert network from the most related previous task. Learn to Grow (Li et al., 2019) uses Differentiable Architecture Search (DARTS (Liu et al., 2019a)) to determine if a layer can be reused, adapted, or renewed (3 fundamental skills: reuse, adapt, new) for a task. Our approach is most closely related to Learn to Grow (Li et al., 2019) which can also be interpreted as a Mixture of Experts framework. Dynamic models have also been explored for efficient transfer learning (Morgado & Vasconcelos, 2019; Guo et al., 2019; Mallya et al., 2018).

Recently, there has been increasing interest in lifelong learning using Vision Transformers (Wang et al., 2022c;b; Xue et al., 2022; Ermis et al., 2022; Douillard et al., 2022; Pelosin et al., 2022; Yu et al., 2021; Li et al., 2022; Iscen et al., 2022; Wang et al., 2022a). *Prompt Based approaches* learn external parameters that encode task-specific information useful for classification (Wang et al., 2022c;a; Douillard et al., 2022). Learning to Prompt (L2P) (Wang et al., 2022c) learns a pool of prompts and uses a key-value based retrieval to infer the task index and retrieve the correct set of prompts at test time. DualPrompt (Wang et al., 2022b) learns generic and task-specific prompts and extends Learning to Prompt. (Xue et al., 2022) uses a ViT pretrained on ImageNet and learns binary masks to enable/disable parameters of the Feedforward Network (FFN), and the attention between image tokens for downstream tasks.

Our Contributions We make four main contributions to the field of lifelong learning with ViTs. (i) We propose and identify Artificial Hippocampi (ArtiHippo) in ViTs, i.e., the final projection layers of the multi-head self-attention blocks in a ViT, to realize a long-term task-similarity-oriented memory mechanism for resilient lifelong learning. We also present a new usage for the class-token in ViTs as the memory growing guidance. (ii) We present a hierarchical task-similarity-oriented, sampling-empowered single-path one-shot neural architecture search method for learning to grow ArtiHippo continually with respect to four basic growing operations: *Skip*, *Reuse*, *Adapt*, and *New*, which not only overcomes catastrophic forgetting, but also leads to efficient forward transfer. (iii) We are the first, to the best of our knowledge, to evaluate lifelong learning with ViTs on the large-scale, diverse and imbalanced VDD benchmark (Rebuffi et al., 2017a) with strong empirical performance obtained. Although the L2P method (Wang et al., 2022c) evaluates on the 5-Datasets benchmark (which contains tasks from diverse domains), each task therein has abundant data and is easy to learn in isolation. In contrast, the VDD dataset contains tasks from varied domains, many of which contain very few labelled samples. (iv) We show that our method is complementary to prompting-based approaches, and combining the two leads to even higher performance.

3 APPROACH

In this section, we first present the ablation study on identifying the ArtiHippo in a Transformer block (Figure 1). Then, we present details of learning to grow ArtiHippo in lifelong learning (Figures 2 and 3).

3.1 IDENTIFYING ARTIHIPPO IN TRANSFORMERS

The left of Figure 1 shows a Vision Transformer (ViT) block (Dosovitskiy et al., 2021). Without loss of generality, denote by $x_{L,d}$ an input sequence consisting of L tokens encoded in a d -dimensional space. In ViTs, the first token is the so-called class-token. The remaining $L - 1$ tokens are formed by patch embedding of an input image, together with additive positional encoding. A Transformer block consists of a MHSA component and a feed-forward network (FFN) with skip/residual connections (He et al., 2016) and layer normalization (LN) (Ba et al., 2016). The FFN is often implemented by a multi-layer perceptron (MLP) with a feature expansion layer MLP^{up} and a feature reduction

layer MLP^{down} . It is defined by,

$$z_{L,d} = x_{L,d} + \text{Proj}(\text{MHSA}(\text{LN}_1(x_{L,d}))), \quad y_{L,d} = z_{L,d} + \text{MLP}^{\text{down}}(\text{MLP}^{\text{up}}(\text{LN}_2(z_{L,d}))), \quad (1)$$

where $\text{Proj}(\cdot)$ is a linear transformation fusing the multi-head outputs from the MHSA module.

The MHSA realizes the dot-product self-attention in h different d_h -dimensional sub-space ($d = h \times d_h$). Each sequence can be rewritten in the multi-head form accordingly, e.g., x_{h,L,d_h} . Let $\bar{X}_{L,d} = \text{LN}_1(X_{L,d})$, and the Query/Key/Value be $Q_{L,d} = \text{Linear}(\bar{X}_{L,d}) \triangleq Q_{h,L,d_h}$, K_{h,L,d_h} and V_{h,L,d_h} . The MHSA is defined by,

$$\text{MHSA}(Q, K, V) = \text{Softmax}\left(\frac{Q \cdot K^T}{\sqrt{d_h}}\right) V \triangleq U_{L,(h,d_h)} \quad (2)$$

where $\text{Softmax}(\cdot)$ is applied along the last dimension of the attention matrix. The projection layer $\text{Proj}(U_{L,(h,d_h)})$ is used to fuse the multi-head information.

For resilient task-incremental lifelong learning using ViTs, **our very first step is to investigate whether there is a simple yet expressive ‘‘sweet spot’’ in the Transformer block that plays the functional role of Hippocampi in the human brain (i.e., ArtiHippo)**, that is converting short-term streaming task memory into long-term memory to support lifelong learning without catastrophic forgetting. The proposed identification process is straightforward. Without introducing any modules handling forgetting, we compare both the task-to-task forward transferrability and the sequential forgetting of different components in a Transformer block. Our intuition is that a desirable ArtiHippo component must enable strong transferrability with manageable forgetting.

To that end, we use the 10 tasks in the VDD benchmark (Rebuffi et al., 2017a). We first compare the transferrability of the ViT trained with the first task, ImageNet to the remaining 9 tasks in a pairwise task-to-task manner and compute the average Top-1 accuracy on the 9 tasks. Then, we start with the ImageNet-trained ViT, and train it on the remaining 9 tasks continually and sequentially in a predefined order with the average forgetting (Chaudhry et al., 2018) on the first 9 tasks (including ImageNet) compared. As shown in Table 1, we compare 11 components or composite components across all blocks in the ImageNet-pretrained ViT.

Denote by T_1, T_2, \dots, T_N a sequence of N tasks (e.g., $N = 10$ in the VDD benchmark). A model consists a feature backbone and a task head classifier. Let $f_{T_{n|1}}$ be the backbone trained for the task n ($n = 2, \dots, N$) with weights warmed-up from the model of task 1, and C_n the learned head classifier from scratch. The average transfer learning accuracy of the first task model to the remaining $N - 1$ tasks is defined by,

$$A_N = \frac{1}{N-1} \sum_{n=2}^N \text{Accuracy}(T_n; f_{T_{n|1}}, C_n), \quad (3)$$

where $\text{Accuracy}(\cdot)$ uses the Top-1 accuracy in classification.

Let $f_{T_{1:n}}$ be the backbone trained sequentially after task T_n and and C_n the head classifier trained for task T_n . Denote by $a_{n,i} = \text{Accuracy}(T_i; f_{T_{1:n}}, C_i)$, the accuracy on the task i using the backbone that has been trained on tasks from 1 to n ($i < n$). The average forgetting on the first $N - 1$ tasks is defined by,

$$\mathbb{F}_N = \frac{1}{N-1} \sum_{n=1}^{N-1} \left(\max_{j \in [n, N-1]} a_{j,n} - a_{N,n} \right), \quad (4)$$

From Table 1, we have a few observations that lead us to identify and select the projection layer as ArtiHippo:

(i) Continually finetuning the entire MHSA block (i.e., MHSA+LN₁) obtains the best average accuracy, which has been observed in (Touvron et al., 2022) in terms of finetuning ImageNet-pretained ViTs on downstream tasks. However, (Touvron et al., 2022) does not consider lifelong learning settings, and as shown here finetuning the entire MHSA block incurs the highest average forgetting, which means that it is task specific.

Index	Finetuned Component	Avg. Accuracy	Avg. Forgetting
1	LN ₁ + LN ₂	81.76	21.24
2	MLP ^{down} + MLP ^{up} + LN ₂	84.20	44.76
3	MLP ^{down}	83.66	37.99
4	LN ₂	80.04	16.35
5	MHSA + LN ₁	85.26	54.38
6	LN ₁	81.18	19.04
7	Query	81.57	19.69
8	Key	81.56	19.19
9	Query+Key	81.49	31.10
10	Value	84.99	37.58
11	Proj (ArtiHippo)	85.11	30.50
Train a Classifier w/ Frozen Backbone		70.78	-

Table 1: Ablation study on identifying the ArtiHippo in a Transformer block (Eqns. 1 and 2). Starting from the first task model from the VDD benchmark, i.e., ImageNet-pretrained ViT, we finetune a given component with other components frozen continually and sequentially across the remaining 9 task in a predefined order, and train the task head classifier from scratch for each individual task. Average Accuracy (Eqn. 3) and Average Forgetting (Eqn. 4) are computed in comparison. The projection layer in the MHSA block is identified and selected as ArtiHippo. The last row shows the result of a conventional transfer learning setting in which the head classifier only is trained.

(ii) Continually finetuning the entire FFN block (i.e., $\text{MLP}^{\text{down}} + \text{MLP}^{\text{up}} + \text{LN}_2$) has a similar effect as finetuning the entire MHSA block. In the literature, the Vision Mixture of Expert framework (Ruiz et al., 2021) where an expert is formed by an entire MLP block takes advantage of the high average performance preservation.

(iii) In lifelong learning scenarios, maintaining either the entire MHSA block or the entire FFN block could address the catastrophic forgetting, but at the expense of high model complexity and heavy computational cost in both learning and inference.

(iv) The final projection layer and the Value layer in the MHSA block, which have been overlooked, can maintain high average accuracy (as well as manageable average forgetting, to be elaborated). It is also much more “affordable” to maintain it in lifelong learning, especially with respect to the four basic growing operations (skip, reuse, adapt and new). Intuitively, the final projection layer is used to fuse multi-head outputs from the self-attention module. In ViTs, the self-attention module is used to mix/fuse tokens spatially and it has been observed in MetaFormers (Yu et al., 2022a;b) that simple local average pooling and even random mixing can perform well. So, it makes sense to keep the self-attention module frozen from the first task (at worst it can play the role of a random mixing operation for a new task) and maintain the projection layer to fuse the outputs. However, the Value layer is implemented as a parallel computation along with the Key and Query, which makes it inefficient to incorporate into the Mixture of Experts framework.

In sum, due to the strong forward transfer ability, maintaining simplicity and for less invasive implementation under the learn-to-grow settings in practice, we select the Projection layer (instead of the Value layer) in the MHSA block as ArtiHippo to develop our proposed long-term task-similarity-oriented memory based lifelong learning. We experimentally show that exploiting the Value layer as the ArtiHippo leads to comparable performance.

3.2 LEARNING TO GROW ARTIHIPPO CONTINUALLY

This section presents details of learning to grow ArtiHippo based on NAS. As illustrated in Figure 2, for a new task t given the network learned for the first $t - 1$ tasks, it consists of three components: the Supernet construction (the parameter space of growing ArtiHippo), the Supernet training (the parameter estimation of growing ArtiHippo), and the target network selection and finetuning (the consolidation of the ArtiHippo for the task t).

3.2.1 SUPERNET CONSTRUCTION

We start with a vanilla D -layer ViT model (e.g., the 12-layer ViT-Base) (Dosovitskiy et al., 2021) and train it on the first task (e.g., ImageNet in the VDD benchmark (Rebuffi et al., 2017a)) following the conventional recipe. The proposed ArtiHippo at the l -th layer in the ViT model consists of a single expert which is defined by a tuple, $E^{l,1} = (P^{l,1}, \mu^{l,1})$, where $P^{l,1}$ is the projection layer and $\mu^{l,1} \in R^d$ is the associated mean class-token pooled from the training dataset after the model is trained. Without loss of generality, we consider how the growing space of ArtiHippo is constructed at a single layer and assume the current ArtiHippo consists of two experts, $\{E^{l,1}, E^{l,2}\}$ (the left in Figure 2).

Inspired by the L2G method (Li et al., 2019), we utilize four operations in the Supernet construction:

- The `skip` operation skips the entire MHSA block (i.e., the hard version of the drop-path method that is widely used in training ViT models), which encourages the adaptivity accounting for the diverse nature of tasks.

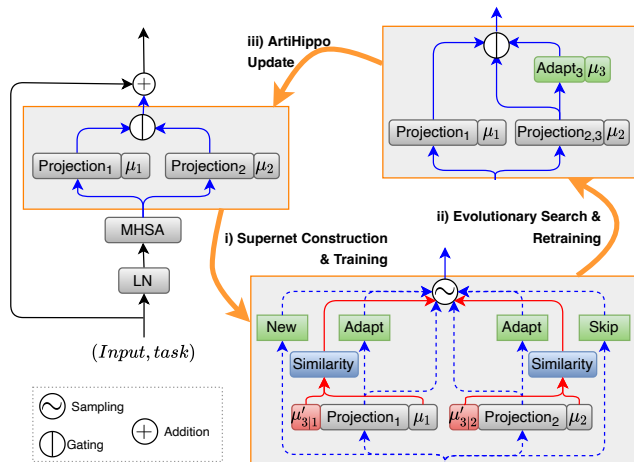


Figure 2: Illustration of ArtiHippo growing via NAS using the four learning-to-grow operations in lifelong learning. The NAS is built on the single-path one-shot (SPOS) formulation (Guo et al., 2020). It consists of two components: Supernet construction and training, and Evolutionary search. Given the current model, the ArtiHippo in a MHSA is represented by a Mixture of Experts and the associated mean class-token (e.g., μ_1 and μ_2). Then, the supernet is constructed using the four operations (illustrated by the dotted arrows in blue). We train the supernet using SPOS with a proposed task-similarity oriented hierarchical exploration-exploitation based sampling method. The task similarity between a new task and old tasks is computed by the normalized cosine similarity between the mean class-tokens, e.g., $(\mu'_{3|1}, \mu_1)$ and $(\mu'_{3|2}, \mu_2)$, (shown by the arrows in red). After the supernet is trained, we use evolutionary search using the same hierarchical exploration-exploitation sampling to seek the target network for the new task. After the evolutionary search, the long-term memory of the new task is maintained (e.g., the newly added Adapt_3 and μ_3). See text for details.

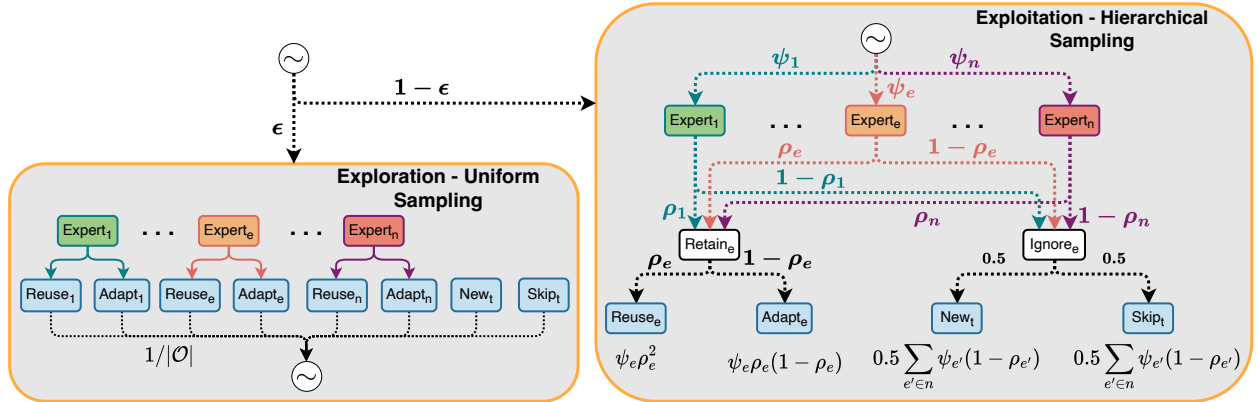


Figure 3: Illustration of the proposed exploration-exploitation sampling strategy used in facilitating the SPOS NAS (Guo et al., 2020) for lifelong learning. It harnesses the best of the vanilla pure exploration strategy (left) and the proposed exploitation strategy (right) using a simple epoch-wise scheduling. See text for details.

- The `reuse` operation exploits the projection layer from an old task for the new task unchanged (including associated mean class-token), which will help task synergies in learning.
- The `adapt` operation introduces a new lightweight layer on top of the projection layer of an old task, implemented by a MLP with one squeezing hidden layer, and a new mean class-token computed at the added adapt MLP layer.
- The `new` operation adds a new projection layer and a mean class-token, enabling the model to handle corner cases and novel situations.

The bottom of Figure 2 shows the growing space. The Supernet is constructed by `reusing` and `adapting` each existing expert at layer l , and adding a new expert and a `skip` expert. The newly added `adapt` MLPs and projection layers will be trained from scratch using the data of a new task only.

How to Adapt in a sustainable way? The proposed `Adapt` operation will effectively increase the depth of the network in a plain way. In the worst case, if too many tasks use `Adapt` on top of each other, we will end up stacking too many MLP layers together. This may lead to unstable training due to gradient vanishing and exploding. Shortcut connections (He et al., 2016) have been shown to alleviate the gradient vanishing and exploding problems, making it possible to train deeper networks. Due to the residual architecture for the adapter layers, the training can ignore an adapter if needed, and leads to a better performance. However, in the lifelong learning setup, where subsequent tasks might have different distributions, the search process might disproportionately encourage `Adapt` operations because of this ability. To counter this, we propose a hybrid `Adapter` which acts as a plain 2-layer MLP during Supernet training and target network selection, and a residual MLP during finetuning. With this hybrid adapter, as we shall show in the ablation study (Table 4), much more compact models can be learned with negligible loss in accuracy.

3.2.2 SUPERNET TRAINING

To train the Supernet constructed for a new task t , many NAS methods can be used such as the DARTS (Liu et al., 2019a) and the more recent single-path one-shot (SPOS) NAS method (Guo et al., 2020). We build on the SPOS method due to its efficiency. The basic idea of SPOS is to sample a single-path sub-network from the Supernet by sampling an expert at every layer in each iteration (mini-batch) of training. One key aspect is the sampling strategy. The vanilla SPOS method uses uniform sampling (i.e., the *pure exploration* strategy, as illustrated in the left of Figure 3), which has the potential of traversing all possible realizations of the mixture of experts of the ArtiHippo in the long run, but may not be desirable (or sufficiently effective) in a lifelong learning setup because it ignores inter-task similarities/synergies.

To overcome this, we propose an exploitation strategy (as illustrated in the right of Figure 3), which utilizes a hierarchical sampling method that forms the categorical distribution over the operations in the search space explicitly based on task similarities. We first present details on the task-similarity oriented sampling in this section. Then we show a simple exploration-exploitation integration strategy to harness the best of the two in Sec. 3.2.4.

Task-Similarity Oriented Sampling: Let \mathbb{E}^l be the set of Experts at the l -th layer learned till task $t - 1$. For each candidate expert $e \in \mathbb{E}^l$, we first compute the mean class-token for the t -task, $\hat{\mu}_e^t$ using the current model, and compute the task similarity between the t -th task and the Expert e ,

$$S_e(t) = \text{NormCosine}(\hat{\mu}_e^t, \mu_e), \quad (5)$$

where $\text{NormCosine}(\cdot, \cdot)$ is the Normalized Cosine Similarity, which is calculated by scaling the Cosine Similarity score between -1 and 1 using the minimum and the maximum scores from all the experts in all the MHSA blocks

of the ViT. This normalization is necessary to increase the difference in magnitudes of the similarities between tasks, which results in better Expert sampling distributions during the sampling process in our experiments.

The categorical distribution is then computed via Softmax across all the scores of all the Experts at a layer. The probability of sampling a candidate Expert $e \in \mathbb{E}^l$ is defined by $\psi_e = \frac{\exp(S_e(t))}{\sum_{e' \in \mathbb{E}^l} \exp(S_{e'}(t))}$. With an Expert e sampled (with a probability ψ_e), we further compute its retention Bernoulli probability via a Sigmoid transformation of the task similarity score defined by $\rho_e = \frac{1}{1 + \exp(-S_e(t))}$.

If the Expert e is retained (with a probability ρ_e), we further use the same Bernoulli probability to sample the two operations, `Reuse` with probability ρ_e and `Adapt` with probability $1 - \rho_e$. If the Expert e is ignored (with probability $1 - \rho_e$), we randomly sample the two operations: `SkIp` and `New` with probability 0.5.

3.2.3 TARGET NETWORK SELECTION AND FINETUNING

After the Supernet is trained, we adopt the same evolutionary search used in the SPOS method (Guo et al., 2020) based on the proposed hierarchical sampling strategy. The evolutionary search is performed on the validation set to select the path which gives the best validation accuracy.

After the target network for a new task is selected, we retrain the newly added layers by the `New` and `Adapt` operations from scratch (random initialization), rather than keeping or warming-up from the weights from the Supernet training. This is based on the observations in network pruning that it is the neural architecture topology that matters and that the warm-up weights may not need to be preserved to ensure good performance on the target dataset (Liu et al., 2019b). We empirically observe this in our experiments as well.

3.2.4 BALANCING EXPLORATION AND EXPLOITATION:

As illustrated in Figure 3, to harness the best of the vanilla pure exploration strategy and the proposed exploitation strategy, we apply epoch-wise exploration and exploitation sampling for simplicity. At the beginning of an epoch in the Supernet training, we choose the pure exploration strategy with a probability of ϵ_1 (e.g., 0.3), and the hierarchical sampling strategy with a probability of $1 - \epsilon_1$. Similarly, when generating the initial population during the evolutionary search, we draw a candidate target network from a uniform distribution over the operations with a probability of ϵ_2 , and from the hierarchical sampling process with a probability of $1 - \epsilon_2$, respectively. In practice, we set $\epsilon_2 > \epsilon_1$ (e.g., $\epsilon_2 = 0.5$) to encourage more exploration during the evolutionary search, while encouraging more exploitation for faster learning in the Supernet training. As we shall show in the experiment, this exploration-exploitation strategy achieves higher Average Accuracy and results in a lower parameter increase than pure exploration.

3.3 INTEGRATING OUR ARTIHIPPO WITH THE LEARN-TO-PROMPT METHOD

As aforementioned, the learn-to-prompt methods (Wang et al., 2022c;b;a; Douillard et al., 2022) are complementary to our proposed learning-to-grow ArtiHippo, we propose a simple method of harnessing the best of the two for resilient lifelong learning. At the beginning of the Supernet training, a task-specific classification token is learned using the ImageNet backbone (similar to S-Prompts (Wang et al., 2022a)). Then, instead of using the `cls` token from the ImageNet task, we used the learned task token during NAS. When finetuning the learned architecture, we first train the task token using the fixed ImageNet backbone, and then use this trained token to train the architecture components. We show that this leads to further improvement.

4 EXPERIMENTS

In this section, we test the proposed method on two benchmarks and compare with the prior art. We evaluate our method in the task-incremental setting, where each task contains a disjoint set of classes and/or domains and task index is available in inference. The proposed method obtains better performance than the prior art in comparisons. **Our PyTorch source code will be released.** Due to space limitations, we provide the implementation details in the Appendix. We use 1 Nvidia Quadro RTX 8000 GPU for all experiments.

Data and Metrics: We evaluate our approach on the Visual Domain Decathlon (VDD) dataset (Rebuffi et al., 2017a) and a sequence of 5 Datasets introduced in (Ebrahimi et al., 2020). Each individual dataset in these two datasets is treated as separate a task with no overlap. The VDD dataset is a challenging benchmark for lifelong learning because of the large variations in tasks as well as small number of samples in many tasks, which makes it a favorable benchmark for lifelong learning. *Details of the two benchmarks are provided in the Appendix.* Since catastrophic forgetting is

Method	ImNet	C100	SVHN	UCF	OGIt	GTSR	DPed	Flwr	Airc.	DTD	Avg. Accuracy
S-Prompts [†] (p=1/task)	82.65	86.69	69.89	51.95	49.55	94.07	99.25	90.39	35.03	56.19	71.57 ± 0.31
L2P [†] (p=12/task)	82.65	89.06	81.43	63.99	62.86	98.21	99.77	94.58	45.00	60.78	77.83 ± 0.28
ArtiHippo (Uniform Sampling)	82.65	85.50	95.63	74.09	82.53	99.93	99.85	79.31	41.62	41.21	78.23 ± 0.93
ArtiHippo (Hierarchical Sampling)	82.65	90.92	95.93	77.08	84.14	99.92	99.80	77.76	47.11	45.79	80.11 ± 1.17
ArtiHippo (Hierarchical Sampling + p=1/task)	82.65	90.99	95.87	78.98	86.12	99.91	99.89	88.20	45.86	51.31	81.98 ± 0.95

Table 2: Results on the VDD benchmark (Rebuffi et al., 2017a). Our method shows clear improvements over the previous approaches. The proposed hierarchical sampling performs better than uniform sampling. All the results from our experiments are averaged over 3 different seeds. The 2 highest accuracies per task have been highlighted. All the methods use the same ViT-B/8 backbone containing 86.04M parameters and having 7.11G FLOPs

fully addressed by our method, we evaluate the the performance of our method using the average accuracy defined by,

$$\mathbf{A}_N = \frac{1}{N} \sum_{i=n}^N a_{N,n}, \quad (6)$$

where N is the total number of tasks, and $a_{n,i} = \text{Accuracy}(T_i; f_{T_{1:n}}, C_i)$ (see Eqn. 3).

Baselines: On the VDD benchmark, we compare with the Learning-to-Prompt (L2P) method (Wang et al., 2022c), which comes closest in terms of evaluating lifelong learning with ViTs on large-scale and diverse tasks and S-Prompts (Wang et al., 2022a). We use our own implementation for evaluating L2P and S-Prompts, and modify the methods to work in the task-incremental setting for fair comparison with our approach, denoted as L2P[†] and S-Prompts[†] in Table 2. We provide the implementation details in the Appendix.

4.1 RESULTS ON THE VDD BENCHMARK

Table 2 shows the results and comparisons. Our method shows consistent performance improvement across tasks compared with ViT based S-Prompts[†] and L2P[†] methods. The gains are particularly significant for tasks with a significantly different distribution than the base ImageNet task (Omniglot, SVHN, UCF101). These results show that introducing new parameters to the base model, as opposed to freezing it and learning external prompts, can improve the performance significantly, which justifies our motivation of seeking more integrative memory mechanisms (Section 1). With the same ViT backbone, our method shows significant improvements over the prompting-based lifelong learning approaches proposed for ViTs (S-Prompts and L2P). However, for tasks which are similar to the base task and have very less data (VGG-Flowers, DTD), the performance of S-Prompts and L2P are better. Thus, prompt-based methods and our growing-based method are complementary and combining them could lead to even better performance. Section 3.3 describes a preliminary approach to combine the two approaches, and Table 2 last row shows that this indeed improves the performance of the proposed ArtiHippo. A more comprehensive integration of ArtiHippo with prompt based approaches is left for future work.

As shown in Table 8 in the Appendix, prompting-based lifelong learning approaches (S-Prompts[†] and L2P[†]) do not perform better than L2G and Adapter, even though they use a better backbone model (ViT-B/8 vs. ResNet26 in L2G). This shows that the gains of our method are because of our parameter growing approach, together with the initial backbone model. The proposed task-similarity oriented sampling procedure outperforms uniform random sampling with lesser number of added parameters (Figure 5 right). This shows that the proposed task-similarity oriented sampling coupled with SPOS NAS (Guo et al., 2020) is effective for lifelong learning with ViTs.

4.2 RESULTS ON THE 5-DATASET BENCHMARK

Table 3 shows the comparisons. We use the same ViT-B/8 backbone pretrained on the ImageNet images from the VDD benchmark for all the experiments across all the methods and upsample the images in the 5-Dataset benchmark (consisting of CIFAR10 (Krizhevsky et al., 2009), MNIST (Lecun et al., 1998), Fashion-MNIST (Xiao et al., 2017), not-MNIST (Bulatov, 2011), and SVHN (Netzer et al., 2011)) to 72×72 . We can see that ArtiHippo significantly outperforms L2P and S-Prompts under the task-incremental setting.

Method	Num. Prompts	Avg. Acc.
S-Prompts [†]	1	91.40
L2P [†]	12	93.76 ± 0.25
ArtiHippo (Projection)	-	96.52 ± 0.4

Table 3: Results on the 5-Dataset benchmark (Ebrahimi et al., 2020). The results have been averaged over 5 different task orders.

4.3 LEARNED ARCHITECTURE AND ARCHITECTURE EFFICIENCY

Figure 4 shows the experts learned for each task in the VDD dataset. When learning CIFAR100 after ImageNet, the search process learns to reuse most of the ImageNet experts. This is an intuitive result since both the tasks represent natural images. In contrast, while learning Omniglot (OGIt, Task 2), the search adds many new experts. Interestingly,

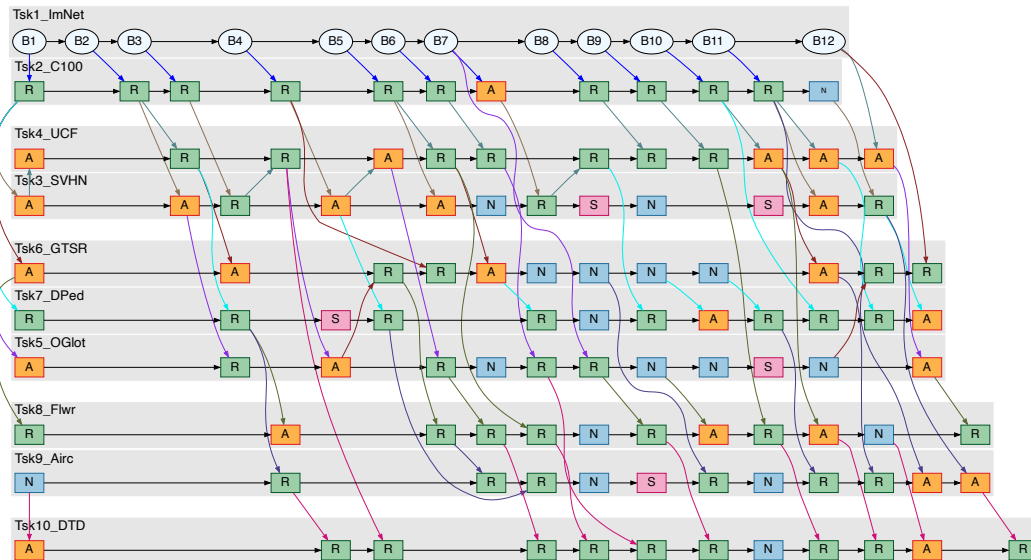


Figure 4: ArtiHippo learned-to-grow on VDD. Starting from the ImageNet-pretrained 12-layer ViT (B1 – B12 in Tsk1_ImNet), sensible architectures are continually learned for the remaining 9 tasks on the VDD dataset. Each column denotes a Transformer block of the ViT in which only the projection layer of the MHSA block is maintained as ArtiHippo in lifelong learning with the remaining components frozen. The proposed Exploration-Exploitation method gradually forms interesting long-term memory structures at different blocks from task to task: some are task specific (e.g., B2 is adapted in SVHN and reused only by Omniglot: two similar tasks) and some have more task synergies (e.g. B3). **S**, **R**, **A** and **N** represents Skip, Reuse, Adapt and New respectively. *Best viewed in color and magnification.*

when learning Omniglot, the search learns to adapt the ImageNet expert in Block 1 and reuse the SVHN expert in Block 2. Both Omniglot and SVHN consist of digit-like images. However, SVHN is in a natural setting, whereas Omniglot contains clean, black and white images. The search process can also use ImageNet experts (experts for natural images) for tasks VGG-Flowers (8th task) and Aircraft (9th task), both of which contain natural images. The sensible architectures learned continually show the effectiveness of the proposed task-similarity-oriented ArtiHippo.

In addition to learning qualitatively meaningful architectures, the proposed method also shows quantitative advantages. On the VDD dataset, because of the `Skip` operation in the proposed framework, the number of parameters *reduces* by 0.92M/task (averaged over 3 different runs). Our method also reduces the number of FLOPs by 0.005G/task (averaged over 3 different runs), which is advantageous as compared to the *increase* of 1.06G/task of the L2P method.

		ImageNet → Omniglot under the lifelong learning setting														
		Adapter in		#Param Added	Rel. ↑	Test Acc.	Learned Operation per Block									
		NAS	Finetune				1	3	5	6	7	8	9	10	11	12
Shortcut in	w/o A & S	w/ A	w/o S	2.96M	3.47%	82.18	A	R	A	R	A	N	N	S	S	
	Adapter	w/ S & A	w/ S & A	4.14M	4.89%	82.32	A	A	A	A	N	A	N	A	N	

Table 4: Results of the ablation study on the Adapter implementation (Sec. 3.2.1): with (w/) vs without (w/o) shortcut connection for the MLP `Adapt` layer. We test lifelong learning from ImageNet to Omniglot in the VDD. The proposed combination of w/o shortcut in Supernet NAS training and target network selection and w/ shortcut in finetuning (retraining newly added layers) is the best in terms of the trade-off between performance and cost.

5 ABLATION STUDIES

5.1 THE STRUCTURE OF Adapter

We verify the effectiveness of the proposed hybrid adapter (Sec. 3.2.1) using a lifelong learning setup with 2 tasks: ImageNet and Omniglot. The Omniglot dataset presents two major challenges for a lifelong learning system. First, Omniglot is a few-shot dataset, for which we may expect a lifelong learning system can learn a model less complex than the one for ImageNet. Second, Omniglot has a significantly different data distribution than ImageNet, for which we may expect a lifelong learning system will need to introduce new parameters, but hopefully in a sensible and

explainable way. Table 4 shows the results. In terms of the learned neural architecture, a more compact model (row 3) is learned without the shortcut in the adapter during Supernet training and target network selection: the last two MHSA blocks are skipped and three blocks are reused. Skipping the last two MHSA blocks makes intuitive sense since Omniglot may not need those high-level self-attention (learned for ImageNet) due to the nature of the dataset. The three consecutive `new` operations (in Blocks 8,9,10) also make sense in terms of learning new self-attention fusion layers (i.e., new memory) to account for the change of the nature of the task. Adding shortcut connection back in the finetuning shows significant performance improvement (from 78.16% to 82.18%), making it very close to the performance (82.32%) obtained by the much more expensive and less intuitively meaningful alternative (the last row).

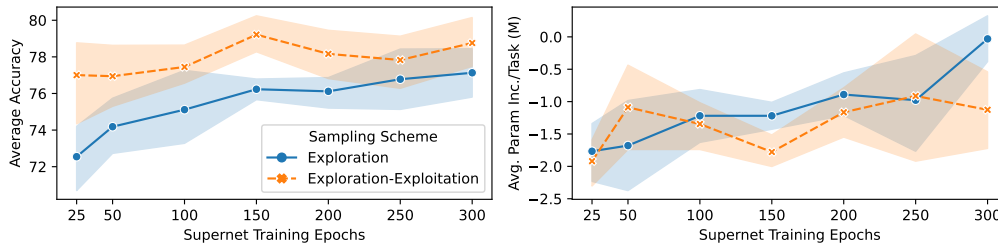


Figure 5: Results of the ablation study on the Exploration-Exploitation (EE) guided sampling in the Supernet NAS training using the VDD benchmark (Rebuffi et al., 2017a). The proposed EE sampling strategy is much more efficient than the pure exploration based strategy (i.e., the vanilla SPOS NAS (Guo et al., 2020)). It uses the Supernet training efficiently even at 25 epochs and achieves better performance than pure Exploration, which is desirable for fast adaptation in dynamic environments using lifelong learning. The % increase in parameters shows that EE strategy is effective in reusing experts from the previous tasks and limiting the increase in parameters. Note that the net increase is negative because the `skip` operation removes the entire attention head. The results have been averaged over 2 task sequences, with 3 runs per sequence with different seeds.

5.2 THE EXPLORATION-EXPLOITATION SAMPLING METHOD

Figure 5, left shows that the proposed exploration-exploitation strategy can consistently obtain higher accuracy than pure exploration even when the supernet is trained a small number of epochs. Although training the supernet for a longer duration improves the accuracy for pure exploration, it also leads to a higher number of parameters in the learned architecture (Figure 5 right). We thus verify that the proposed exploration-exploitation strategy is effective and efficient. This also shows that proposed task-similarity metric is meaningful.

Component	ImNet	C100	SVHN	UCF	OGIt	GTSR	DPed	Flwr	Airc.	DTD	Avg. Accuracy
Projection	82.65	90.92	95.93	77.08	84.14	99.92	99.80	77.76	47.11	45.79	80.11 ± 1.17
Value	82.65	84.98	95.74	76.25	83.55	99.93	99.90	84.80	44.97	49.80	80.26 ± 1.62
Query	82.65	89.47	94.09	68.85	75.71	99.86	99.91	77.81	34.51	51.47	77.43 ± 0.43
FFN	82.65	90.92	94.95	68.02	70.16	99.91	99.63	63.37	18.85	29.70	71.82 ± 1.80

Table 5: Results of ablation study on the other components of the ViT used for realizing the ArtiHippo. Realizing ArtiHippo at the Value shows slightly better performance than the Projection layer. However, the Value layer is often coupled with the Query and Key layers for efficient computation. Using the Projection layer offers negligible drop in Average Accuracy without sacrificing efficiency. * The results averaged over 3 different seeds.

5.3 EVALUATING FEASIBILITY OF OTHER ViT COMPONENTS AS ARTIHIPPO

Table 5 shows the accuracy with other components if the ViT used for learning the Mixture of Experts using the proposed NAS method. Interestingly, the Value performs slightly better than the Projection layer. However, using the the Value layer would be inefficient, as it is implemented as a parallel linear layer with the Query and Key. The projection layer can be efficiently replaced with the Mixture of Experts framework. Table 5 also shows that the Query component from the MHSA block, and the FFN which is typically used in the Mixture of Experts framework for Transformers (Ruiz et al., 2021), are ill suited. This reinforces our identification of the ArtiHippo in Section 3.1.

6 CONCLUSIONS

This paper presents a method of learning to grow Artificial Hippocampi (ArtiHippo) in Vision Transformers for resilient lifelong learning. The final projection layers in the Multi-Head Self-Attention blocks of a Vision Transformer are identified and selected as “Hippocampi” to implement long-term task-similarity-oriented memory in lifelong learning. The ArtiHippo is maintained by a proposed hierarchical task-similarity-oriented sampling based single-path one-shot Neural Architecture Search algorithm with exploration and exploitation handled in the sampling. The NAS space

of ArtiHippo is defined by four basic learning-to-grow operations: Skip, Reuse, Adapt and New, with the Adapt realized with a hybrid Adapter. The task similarity is defined by the normalized cosine similarity between the mean class-tokens of a new task and old tasks. In experiments, the proposed method is tested on the challenging VDD and the 5-Datasets benchmarks. It obtains better performance than the prior art with sensible ArtiHippo learned continually.

ACKNOWLEDGEMENTS

This research is partly supported by NSF IIS-1909644, ARO Grant W911NF1810295, ARO Grant W911NF2210010, NSF IIS-1822477, NSF CMMI-2024688, NSF IUSE-2013451 and DHHS-ACL Grant 90IFDV0017-01-00. The views and conclusions contained herein are those of the authors and should not be interpreted as necessarily representing the official policies or endorsements, either expressed or implied, of the NSF, ARO, DHHS or the U.S. Government. The U.S. Government is authorized to reproduce and distribute reprints for Governmental purposes not withstanding any copyright annotation thereon.

REFERENCES

- Rahaf Aljundi, Punarjay Chakravarty, and Tinne Tuytelaars. Expert gate: Lifelong learning with a network of experts. In *Proceedings of the IEEE Conference on Computer Vision and Pattern Recognition (CVPR)*, July 2017.
- Rahaf Aljundi, Francesca Babiloni, Mohamed Elhoseiny, Marcus Rohrbach, and Tinne Tuytelaars. Memory aware synapses: Learning what (not) to forget. In Vittorio Ferrari, Martial Hebert, Cristian Sminchisescu, and Yair Weiss (eds.), *Computer Vision – ECCV 2018*, pp. 144–161, Cham, 2018. Springer International Publishing. ISBN 978-3-030-01219-9.
- Rahaf Aljundi, Eugene Belilovsky, Tinne Tuytelaars, Laurent Charlin, Massimo Caccia, Min Lin, and Lucas Page-Caccia. Online continual learning with maximal interfered retrieval. In H. Wallach, H. Larochelle, A. Beygelzimer, F. d'Alché-Buc, E. Fox, and R. Garnett (eds.), *Advances in Neural Information Processing Systems*, volume 32. Curran Associates, Inc., 2019a. URL <https://proceedings.neurips.cc/paper/2019/file/15825aee15eb335cc13f9b559f166ee8-Paper.pdf>.
- Rahaf Aljundi, Min Lin, Baptiste Goujaud, and Yoshua Bengio. Gradient based sample selection for online continual learning. In H. Wallach, H. Larochelle, A. Beygelzimer, F. d'Alché-Buc, E. Fox, and R. Garnett (eds.), *Advances in Neural Information Processing Systems*, volume 32. Curran Associates, Inc., 2019b. URL <https://proceedings.neurips.cc/paper/2019/file/e562cd9c0768d5464b64cf61da7fc6bb-Paper.pdf>.
- Rahaf Aljundi, Marcus Rohrbach, and Tinne Tuytelaars. Selfless sequential learning. In *International Conference on Learning Representations*, 2019c. URL <https://openreview.net/forum?id=Bkxbrn0cYX>.
- Jimmy Lei Ba, Jamie Ryan Kiros, and Geoffrey E Hinton. Layer normalization. *arXiv preprint arXiv:1607.06450*, 2016.
- Yogesh Balaji, Mehrdad Farajtabar, Dong Yin, Alex Mott, and Ang Li. The effectiveness of memory replay in large scale continual learning. *arXiv preprint arXiv:2010.02418*, 2020.
- Jihwan Bang, Heesu Kim, YoungJoon Yoo, Jung-Woo Ha, and Jonghyun Choi. Rainbow memory: Continual learning with a memory of diverse samples. In *Proceedings of the IEEE/CVF Conference on Computer Vision and Pattern Recognition (CVPR)*, pp. 8218–8227, June 2021.
- Hakan Bilen, Basura Fernando, Efstratios Gavves, Andrea Vedaldi, and Stephen Gould. Dynamic image networks for action recognition. In *2016 IEEE Conference on Computer Vision and Pattern Recognition (CVPR)*, pp. 3034–3042, 2016. doi: 10.1109/CVPR.2016.331.
- Rishi Bommasani, Drew A Hudson, Ehsan Adeli, Russ Altman, Simran Arora, Sydney von Arx, Michael S Bernstein, Jeannette Bohg, Antoine Bosselut, Emma Brunskill, et al. On the opportunities and risks of foundation models. *arXiv preprint arXiv:2108.07258*, 2021.
- Yaroslav Bulatov. notmnist dataset. <http://yaroslavvb.blogspot.com/2011/09/notmnist-dataset.html>, 2011.

- Pietro Buzzega, Matteo Boschini, Angelo Porrello, Davide Abati, and SIMONE CALDERARA. Dark experience for general continual learning: a strong, simple baseline. In H. Larochelle, M. Ranzato, R. Hadsell, M.F. Balcan, and H. Lin (eds.), *Advances in Neural Information Processing Systems*, volume 33, pp. 15920–15930. Curran Associates, Inc., 2020. URL <https://proceedings.neurips.cc/paper/2020/file/b704ea2c39778f07c617f6b7ce480e9e-Paper.pdf>.
- Hyuntak Cha, Jaeho Lee, and Jinwoo Shin. Co2l: Contrastive continual learning. In *Proceedings of the IEEE/CVF International Conference on Computer Vision (ICCV)*, pp. 9516–9525, October 2021.
- Arslan Chaudhry, Puneet K. Dokania, Thalayasingam Ajanthan, and Philip H. S. Torr. Riemannian walk for incremental learning: Understanding forgetting and intransigence. In Vittorio Ferrari, Martial Hebert, Cristian Sminchisescu, and Yair Weiss (eds.), *Computer Vision – ECCV 2018*, pp. 556–572, Cham, 2018. Springer International Publishing. ISBN 978-3-030-01252-6.
- Arslan Chaudhry, Marc’Aurelio Ranzato, Marcus Rohrbach, and Mohamed Elhoseiny. Efficient lifelong learning with A-GEM. In *7th International Conference on Learning Representations, ICLR 2019, New Orleans, LA, USA, May 6-9, 2019*. OpenReview.net, 2019a. URL https://openreview.net/forum?id=Hkf2_sC5FX.
- Arslan Chaudhry, Marcus Rohrbach, Mohamed Elhoseiny, Thalayasingam Ajanthan, Puneet K Dokania, Philip HS Torr, and Marc’Aurelio Ranzato. On tiny episodic memories in continual learning. *arXiv preprint arXiv:1902.10486*, 2019b.
- Arslan Chaudhry, Albert Gordo, Puneet Dokania, Philip Torr, and David Lopez-Paz. Using hindsight to anchor past knowledge in continual learning. *Proceedings of the AAAI Conference on Artificial Intelligence*, 35(8):6993–7001, May 2021. doi: 10.1609/aaai.v35i8.16861. URL <https://ojs.aaai.org/index.php/AAAI/article/view/16861>.
- Thomas B Christophel, P Christiaan Klink, Bernhard Spitzer, Pieter R Roelfsema, and John-Dylan Haynes. The distributed nature of working memory. *Trends in cognitive sciences*, 21(2):111–124, 2017.
- Mircea Cimpoi, Subhansu Maji, Iasonas Kokkinos, Sammy Mohamed, and Andrea Vedaldi. Describing textures in the wild. In *2014 IEEE Conference on Computer Vision and Pattern Recognition*, pp. 3606–3613, 2014. doi: 10.1109/CVPR.2014.461.
- Yulai Cong, Miaoyun Zhao, Jianqiao Li, Sijia Wang, and Lawrence Carin. Gan memory with no forgetting. In H. Larochelle, M. Ranzato, R. Hadsell, M.F. Balcan, and H. Lin (eds.), *Advances in Neural Information Processing Systems*, volume 33, pp. 16481–16494. Curran Associates, Inc., 2020. URL <https://proceedings.neurips.cc/paper/2020/file/bf201d5407a6509fa536afc4b380577e-Paper.pdf>.
- Matthias De Lange and Tinne Tuytelaars. Continual prototype evolution: Learning online from non-stationary data streams. In *2021 IEEE/CVF International Conference on Computer Vision (ICCV)*, pp. 8230–8239, 2021. doi: 10.1109/ICCV48922.2021.00814.
- Alexey Dosovitskiy, Lucas Beyer, Alexander Kolesnikov, Dirk Weissenborn, Xiaohua Zhai, Thomas Unterthiner, Mostafa Dehghani, Matthias Minderer, Georg Heigold, Sylvain Gelly, Jakob Uszkoreit, and Neil Houlsby. An image is worth 16x16 words: Transformers for image recognition at scale. In *International Conference on Learning Representations*, 2021. URL <https://openreview.net/forum?id=YicbFdNTTy>.
- Arthur Douillard, Matthieu Cord, Charles Ollion, Thomas Robert, and Eduardo Valle. Podnet: Pooled outputs distillation for small-tasks incremental learning. In Andrea Vedaldi, Horst Bischof, Thomas Brox, and Jan-Michael Frahm (eds.), *Computer Vision – ECCV 2020*, pp. 86–102, Cham, 2020. Springer International Publishing. ISBN 978-3-030-58565-5.
- Arthur Douillard, Alexandre Ramé, Guillaume Couairon, and Matthieu Cord. Dytox: Transformers for continual learning with dynamic token expansion. In *Proceedings of the IEEE/CVF Conference on Computer Vision and Pattern Recognition (CVPR)*, pp. 9285–9295, June 2022.
- Sayna Ebrahimi, Franziska Meier, Roberto Calandra, Trevor Darrell, and Marcus Rohrbach. Adversarial continual learning. In Andrea Vedaldi, Horst Bischof, Thomas Brox, and Jan-Michael Frahm (eds.), *Computer Vision – ECCV 2020*, pp. 386–402, Cham, 2020. Springer International Publishing. ISBN 978-3-030-58621-8.
- Beyza Ermis, Giovanni Zappella, Martin Wistuba, Aditya Rawal, and Cédric Archambeau. Continual learning with transformers for image classification. In *Proceedings of the IEEE/CVF Conference on Computer Vision and Pattern Recognition (CVPR) Workshops*, pp. 3774–3781, June 2022.

- Chrisantha Fernando, Dylan Banarse, Charles Blundell, Yori Zwols, David Ha, Andrei A Rusu, Alexander Pritzel, and Daan Wierstra. Pathnet: Evolution channels gradient descent in super neural networks. *arXiv preprint arXiv:1701.08734*, 2017.
- Yunhui Guo, Honghui Shi, Abhishek Kumar, Kristen Grauman, Tajana Rosing, and Rogerio Feris. Spottune: Transfer learning through adaptive fine-tuning. In *Proceedings of the IEEE/CVF Conference on Computer Vision and Pattern Recognition (CVPR)*, June 2019.
- Zichao Guo, Xiangyu Zhang, Haoyuan Mu, Wen Heng, Zechun Liu, Yichen Wei, and Jian Sun. Single path one-shot neural architecture search with uniform sampling. In Andrea Vedaldi, Horst Bischof, Thomas Brox, and Jan-Michael Frahm (eds.), *Computer Vision – ECCV 2020*, pp. 544–560, Cham, 2020. Springer International Publishing. ISBN 978-3-030-58517-4.
- Tyler L. Hayes, Nathan D. Cahill, and Christopher Kanan. Memory efficient experience replay for streaming learning. In *2019 International Conference on Robotics and Automation (ICRA)*, pp. 9769–9776, 2019. doi: 10.1109/ICRA.2019.8793982.
- Tyler L. Hayes, Kushal Kafle, Robik Shrestha, Manoj Acharya, and Christopher Kanan. Remind your neural network to prevent catastrophic forgetting. In Andrea Vedaldi, Horst Bischof, Thomas Brox, and Jan-Michael Frahm (eds.), *Computer Vision – ECCV 2020*, pp. 466–483, Cham, 2020. Springer International Publishing. ISBN 978-3-030-58598-3.
- Kaiming He, Xiangyu Zhang, Shaoqing Ren, and Jian Sun. Deep residual learning for image recognition. In *Proceedings of the IEEE Conference on Computer Vision and Pattern Recognition (CVPR)*, June 2016.
- Ahmet Iscen, Thomas Bird, Mathilde Caron, Alireza Fathi, and Cordelia Schmid. A memory transformer network for incremental learning. *arXiv preprint arXiv:2210.04485*, 2022.
- Diederik P. Kingma and Jimmy Ba. Adam: A method for stochastic optimization, 2014. URL <https://arxiv.org/abs/1412.6980>.
- James Kirkpatrick, Razvan Pascanu, Neil Rabinowitz, Joel Veness, Guillaume Desjardins, Andrei A. Rusu, Kieran Milan, John Quan, Tiago Ramalho, Agnieszka Grabska-Barwinska, Demis Hassabis, Claudia Clopath, Dharshan Kumaran, and Raia Hadsell. Overcoming catastrophic forgetting in neural networks. *Proceedings of the National Academy of Sciences*, 114(13):3521–3526, 2017. doi: 10.1073/pnas.1611835114. URL <https://www.pnas.org/doi/abs/10.1073/pnas.1611835114>.
- Alex Krizhevsky, Geoffrey Hinton, et al. Learning multiple layers of features from tiny images. 2009.
- Brenden M. Lake, Ruslan Salakhutdinov, and Joshua B. Tenenbaum. Human-level concept learning through probabilistic program induction. *Science*, 350(6266):1332–1338, 2015. doi: 10.1126/science.aab3050. URL <https://www.science.org/doi/abs/10.1126/science.aab3050>.
- Y. Lecun, L. Bottou, Y. Bengio, and P. Haffner. Gradient-based learning applied to document recognition. *Proceedings of the IEEE*, 86(11):2278–2324, 1998. doi: 10.1109/5.726791.
- Duo Li, Guimei Cao, Yunlu Xu, Zhanzhan Cheng, and Yi Niu. Technical report for iccv 2021 challenge sslad-track3b: Transformers are better continual learners. *arXiv preprint arXiv:2201.04924*, 2022.
- Xilai Li, Yingbo Zhou, Tianfu Wu, Richard Socher, and Caiming Xiong. Learn to grow: A continual structure learning framework for overcoming catastrophic forgetting. In Kamalika Chaudhuri and Ruslan Salakhutdinov (eds.), *Proceedings of the 36th International Conference on Machine Learning, ICML 2019, 9-15 June 2019, Long Beach, California, USA*, volume 97 of *Proceedings of Machine Learning Research*, pp. 3925–3934. PMLR, 2019. URL <http://proceedings.mlr.press/v97/li19m.html>.
- Zhizhong Li and Derek Hoiem. Learning without forgetting. *IEEE Transactions on Pattern Analysis and Machine Intelligence*, 40(12):2935–2947, 2018. doi: 10.1109/TPAMI.2017.2773081.
- Hanxiao Liu, Karen Simonyan, and Yiming Yang. DARTS: Differentiable architecture search. In *International Conference on Learning Representations*, 2019a. URL <https://openreview.net/forum?id=S1eYHoC5FX>.
- Zhuang Liu, Mingjie Sun, Tinghui Zhou, Gao Huang, and Trevor Darrell. Rethinking the value of network pruning. In *7th International Conference on Learning Representations, ICLR 2019, New Orleans, LA, USA, May 6-9, 2019*. OpenReview.net, 2019b. URL <https://openreview.net/forum?id=rJlnB3C5Ym>.

- David Lopez-Paz and Marc' Aurelio Ranzato. Gradient episodic memory for continual learning. In I. Guyon, U. Von Luxburg, S. Bengio, H. Wallach, R. Fergus, S. Vishwanathan, and R. Garnett (eds.), *Advances in Neural Information Processing Systems*, volume 30. Curran Associates, Inc., 2017. URL <https://proceedings.neurips.cc/paper/2017/file/f87522788a2be2d171666752f97ddeb-Paper.pdf>.
- S. Maji, J. Kannala, E. Rahtu, M. Blaschko, and A. Vedaldi. Fine-grained visual classification of aircraft. Technical report, 2013.
- Arun Mallya, Dillon Davis, and Svetlana Lazebnik. Piggyback: Adapting a single network to multiple tasks by learning to mask weights. In *Proceedings of the European Conference on Computer Vision (ECCV)*, September 2018.
- Michael McCloskey and Neal J. Cohen. Catastrophic interference in connectionist networks: The sequential learning problem. volume 24 of *Psychology of Learning and Motivation*, pp. 109–165. Academic Press, 1989. doi: [https://doi.org/10.1016/S0079-7421\(08\)60536-8](https://doi.org/10.1016/S0079-7421(08)60536-8). URL <https://www.sciencedirect.com/science/article/pii/S0079742108605368>.
- Pedro Morgado and Nuno Vasconcelos. Nettare: Tuning the architecture, not just the weights. In *Proceedings of the IEEE/CVF Conference on Computer Vision and Pattern Recognition (CVPR)*, June 2019.
- S. Munder and D.M. Gavrilu. An experimental study on pedestrian classification. *IEEE Transactions on Pattern Analysis and Machine Intelligence*, 28(11):1863–1868, 2006. doi: 10.1109/TPAMI.2006.217.
- Yuval Netzer, Tao Wang, Adam Coates, Alessandro Bissacco, Bo Wu, and Andrew Y. Ng. Reading digits in natural images with unsupervised feature learning. In *NIPS Workshop on Deep Learning and Unsupervised Feature Learning 2011*, 2011. URL http://ufldl.stanford.edu/housenumbers/nips2011_housenumbers.pdf.
- Cuong V. Nguyen, Yingzhen Li, Thang D. Bui, and Richard E. Turner. Variational continual learning. In *International Conference on Learning Representations*, 2018. URL <https://openreview.net/forum?id=BkQqq0gRb>.
- Maria-Elena Nilsback and Andrew Zisserman. Automated flower classification over a large number of classes. In *2008 Sixth Indian Conference on Computer Vision, Graphics & Image Processing*, pp. 722–729, 2008. doi: 10.1109/ICVGIP.2008.47.
- Francesco Pelosin, Saurav Jha, Andrea Torsello, Bogdan Raducanu, and Joost van de Weijer. Towards exemplar-free continual learning in vision transformers: An account of attention, functional and weight regularization. In *Proceedings of the IEEE/CVF Conference on Computer Vision and Pattern Recognition (CVPR) Workshops*, pp. 3820–3829, June 2022.
- Quang Pham, Chenghao Liu, and Steven Hoi. Dualnet: Continual learning, fast and slow. In M. Ranzato, A. Beygelzimer, Y. Dauphin, P.S. Liang, and J. Wortman Vaughan (eds.), *Advances in Neural Information Processing Systems*, volume 34, pp. 16131–16144. Curran Associates, Inc., 2021. URL <https://proceedings.neurips.cc/paper/2021/file/86a1fa88adb5c33bd7a68ac2f9f3f96b-Paper.pdf>.
- Ameya Prabhu, Philip H. S. Torr, and Puneet K. Dokania. Gdumb: A simple approach that questions our progress in continual learning. In Andrea Vedaldi, Horst Bischof, Thomas Brox, and Jan-Michael Frahm (eds.), *Computer Vision – ECCV 2020*, pp. 524–540, Cham, 2020. Springer International Publishing. ISBN 978-3-030-58536-5.
- Alec Radford, Jong Wook Kim, Chris Hallacy, Aditya Ramesh, Gabriel Goh, Sandhini Agarwal, Girish Sastry, Amanda Askell, Pamela Mishkin, Jack Clark, Gretchen Krueger, and Ilya Sutskever. Learning transferable visual models from natural language supervision. In Marina Meila and Tong Zhang (eds.), *Proceedings of the 38th International Conference on Machine Learning*, volume 139 of *Proceedings of Machine Learning Research*, pp. 8748–8763. PMLR, 18–24 Jul 2021. URL <https://proceedings.mlr.press/v139/radford21a.html>.
- Esteban Real, Alok Aggarwal, Yanping Huang, and Quoc V Le. Regularized evolution for image classifier architecture search. In *Proceedings of the aaai conference on artificial intelligence*, volume 33, pp. 4780–4789, 2019.
- Sylvestre-Alvise Rebuffi, Hakan Bilen, and Andrea Vedaldi. Learning multiple visual domains with residual adapters. In I. Guyon, U. Von Luxburg, S. Bengio, H. Wallach, R. Fergus, S. Vishwanathan, and R. Garnett (eds.), *Advances in Neural Information Processing Systems*, volume 30. Curran Associates, Inc., 2017a. URL <https://proceedings.neurips.cc/paper/2017/file/e7b24b112a44fdd9ee93bdf998c6ca0e-Paper.pdf>.

- Sylvestre-Alvise Rebuffi, Alexander Kolesnikov, Georg Sperl, and Christoph H. Lampert. icarl: Incremental classifier and representation learning. In *Proceedings of the IEEE Conference on Computer Vision and Pattern Recognition (CVPR)*, July 2017b.
- Carlos Riquelme Ruiz, Joan Puigcerver, Basil Mustafa, Maxim Neumann, Rodolphe Jenatton, André Susano Pinto, Daniel Keysers, and Neil Houlsby. Scaling vision with sparse mixture of experts. In A. Beygelzimer, Y. Dauphin, P. Liang, and J. Wortman Vaughan (eds.), *Advances in Neural Information Processing Systems*, 2021. URL https://openreview.net/forum?id=NGPmH3vbAA_.
- Olga Russakovsky, Jia Deng, Hao Su, Jonathan Krause, Sanjeev Satheesh, Sean Ma, Zhiheng Huang, Andrej Karpathy, Aditya Khosla, Michael Bernstein, Alexander C. Berg, and Li Fei-Fei. ImageNet Large Scale Visual Recognition Challenge. *International Journal of Computer Vision (IJCV)*, 115(3):211–252, 2015. doi: 10.1007/s11263-015-0816-y.
- Andrei A Rusu, Neil C Rabinowitz, Guillaume Desjardins, Hubert Soyer, James Kirkpatrick, Koray Kavukcuoglu, Razvan Pascanu, and Raia Hadsell. Progressive neural networks. *arXiv preprint arXiv:1606.04671*, 2016.
- Jonathan Schwarz, Wojciech Czarnecki, Jelena Luketina, Agnieszka Grabska-Barwinska, Yee Whye Teh, Razvan Pascanu, and Raia Hadsell. Progress & compress: A scalable framework for continual learning. In Jennifer Dy and Andreas Krause (eds.), *Proceedings of the 35th International Conference on Machine Learning*, volume 80 of *Proceedings of Machine Learning Research*, pp. 4528–4537. PMLR, 10–15 Jul 2018. URL <https://proceedings.mlr.press/v80/schwarz18a.html>.
- Hanul Shin, Jung Kwon Lee, Jaehong Kim, and Jiwon Kim. Continual learning with deep generative replay. In I. Guyon, U. Von Luxburg, S. Bengio, H. Wallach, R. Fergus, S. Vishwanathan, and R. Garnett (eds.), *Advances in Neural Information Processing Systems*, volume 30. Curran Associates, Inc., 2017. URL <https://proceedings.neurips.cc/paper/2017/file/0efbe98067c6c73dba1250d2beaa81f9-Paper.pdf>.
- Khurram Soomro, Amir Roshan Zamir, and Mubarak Shah. UCF101: A dataset of 101 human actions classes from videos in the wild. *CoRR*, abs/1212.0402, 2012. URL <http://arxiv.org/abs/1212.0402>.
- J. Stallkamp, M. Schlipsing, J. Salmen, and C. Igel. Man vs. computer: Benchmarking machine learning algorithms for traffic sign recognition. *Neural Networks*, 32:323–332, 2012. ISSN 0893-6080. doi: <https://doi.org/10.1016/j.neunet.2012.02.016>. URL <https://www.sciencedirect.com/science/article/pii/S0893608012000457>. Selected Papers from IJCNN 2011.
- Sebastian Thrun and Tom M. Mitchell. Lifelong robot learning. *Robotics and Autonomous Systems*, 15(1):25–46, 1995. ISSN 0921-8890. doi: [https://doi.org/10.1016/0921-8890\(95\)00004-Y](https://doi.org/10.1016/0921-8890(95)00004-Y). URL <https://www.sciencedirect.com/science/article/pii/092188909500004Y>. The Biology and Technology of Intelligent Autonomous Agents.
- Hugo Touvron, Matthieu Cord, Alaaeldin El-Nouby, Jakob Verbeek, and Hervé Jégou. Three things everyone should know about vision transformers. *arXiv preprint arXiv:2203.09795*, 2022.
- Ashish Vaswani, Noam Shazeer, Niki Parmar, Jakob Uszkoreit, Llion Jones, Aidan N Gomez, Łukasz Kaiser, and Illia Polosukhin. Attention is all you need. In I. Guyon, U. Von Luxburg, S. Bengio, H. Wallach, R. Fergus, S. Vishwanathan, and R. Garnett (eds.), *Advances in Neural Information Processing Systems*, volume 30. Curran Associates, Inc., 2017. URL <https://proceedings.neurips.cc/paper/2017/file/3f5ee243547dee91fbd053c1c4a845aa-Paper.pdf>.
- Ivan Voito and Thomas D Mrsic-Flogel. Cortical feedback loops bind distributed representations of working memory. *Nature*, 608(7922):381–389, 2022.
- Yabin Wang, Zhiwu Huang, and Xiaopeng Hong. S-prompts learning with pre-trained transformers: An occam’s razor for domain incremental learning. *arXiv preprint arXiv:2207.12819*, 2022a.
- Zifeng Wang, Zizhao Zhang, Sayna Ebrahimi, Ruoxi Sun, Han Zhang, Chen-Yu Lee, Xiaoqi Ren, Guolong Su, Vincent Perot, Jennifer Dy, and Tomas Pfister. Dualprompt: Complementary prompting for rehearsal-free continual learning, 2022b. URL <https://arxiv.org/abs/2204.04799>.
- Zifeng Wang, Zizhao Zhang, Chen-Yu Lee, Han Zhang, Ruoxi Sun, Xiaoqi Ren, Guolong Su, Vincent Perot, Jennifer Dy, and Tomas Pfister. Learning to prompt for continual learning. In *Proceedings of the IEEE/CVF Conference on Computer Vision and Pattern Recognition (CVPR)*, pp. 139–149, June 2022c.

- Ross Wightman. Pytorch image models. <https://github.com/rwightman/pytorch-image-models>, 2019.
- Yue Wu, Yinpeng Chen, Lijuan Wang, Yuancheng Ye, Zicheng Liu, Yandong Guo, and Yun Fu. Large scale incremental learning. In *Proceedings of the IEEE/CVF Conference on Computer Vision and Pattern Recognition (CVPR)*, June 2019.
- Han Xiao, Kashif Rasul, and Roland Vollgraf. Fashion-mnist: a novel image dataset for benchmarking machine learning algorithms. *arXiv preprint arXiv:1708.07747*, 2017.
- Mengqi Xue, Haofei Zhang, Jie Song, and Mingli Song. Meta-attention for vit-backed continual learning. In *Proceedings of the IEEE/CVF Conference on Computer Vision and Pattern Recognition (CVPR)*, pp. 150–159, June 2022.
- Jaehong Yoon, Eunho Yang, Jeongtae Lee, and Sung Ju Hwang. Lifelong learning with dynamically expandable networks. In *International Conference on Learning Representations*, 2018. URL <https://openreview.net/forum?id=Sk7KsfW0->.
- Pei Yu, Yinpeng Chen, Ying Jin, and Zicheng Liu. Improving vision transformers for incremental learning. *arXiv preprint arXiv:2112.06103*, 2021.
- Weihao Yu, Mi Luo, Pan Zhou, Chenyang Si, Yichen Zhou, Xinchao Wang, Jiashi Feng, and Shuicheng Yan. Metaformer is actually what you need for vision. In *Proceedings of the IEEE/CVF Conference on Computer Vision and Pattern Recognition*, pp. 10819–10829, 2022a.
- Weihao Yu, Chenyang Si, Pan Zhou, Mi Luo, Yichen Zhou, Jiashi Feng, Shuicheng Yan, and Xinchao Wang. Metaformer baselines for vision. *arXiv preprint arXiv:2210.13452*, 2022b.
- Friedemann Zenke, Ben Poole, and Surya Ganguli. Continual learning through synaptic intelligence. In Doina Precup and Yee Whye Teh (eds.), *Proceedings of the 34th International Conference on Machine Learning*, volume 70 of *Proceedings of Machine Learning Research*, pp. 3987–3995. PMLR, 06–11 Aug 2017. URL <https://proceedings.mlr.press/v70/zenke17a.html>.

A OVERVIEW

In the Appendix, we elaborate on the following aspects that are not presented in the submission due to space limit:

- *Details of the two benchmarks:* the Visual Domain Decathlon (VDD) (Rebuffi et al., 2017a) benchmark (Sec. B.1) and the 5-Datasets (Ebrahimi et al., 2020) benchmark (Sec. B.2).
- *The Base Model and Its Training Details:* the Vision Transformer (ViT) model specification (ViT-B/8) used in our experiments (Sec. C), and training details on the ImageNet (Sec. D).
- *Background:* To be self-contained, we give a brief introduction to the learn-to-grow method (Li et al., 2019) in Sec. E and the single-path one-shot (SPOS) neural architecture search (NAS) algorithm (Guo et al., 2020) in Sec. G.
- *Comparison of Learn to Prompt, S-Prompts and ArtiHippo with Learn to Grow:* In Section F, we compare the performance of L2P[†] (Wang et al., 2022c), S-Prompts[†], and the proposed ArtiHippo with Learn to Grow on the VDD benchmark. We show that even with a stronger backbone model (ViT-B/8 instead of ResNet26 used in Learn to Grow), S-Prompts[†] performs significantly worse, and L2P[†] shows marginal improvements. ArtiHippo can outperform Learn to Grow by taking advantage of a strong backbone along with the proposed task-similarity oriented NAS.
- *Modifying Learn to Prompt and S-Prompts for task-incremental setting:* In Section H, we describe our implementation of L2p[†] and S-Prompts[†] used for comparisons.
- *Settings and Hyperparameters in the Proposed Lifelong Learning:* We provide them in Sec. I, together with the breakdown of results of 5 different sequences of task orders tested in the VDD benchmark and the corresponding ArtiHippo learned-to-grow with respect the different task orders.
- *Learned architecture with pure exploration and different task order:* We show that with a different task order, the proposed method can still learn to exploit inter-task similarities. We also show that pure exploration cannot effectively exploit task similarities by comparing the learned architecture with the architecture learned using the exploration-exploitation strategy.

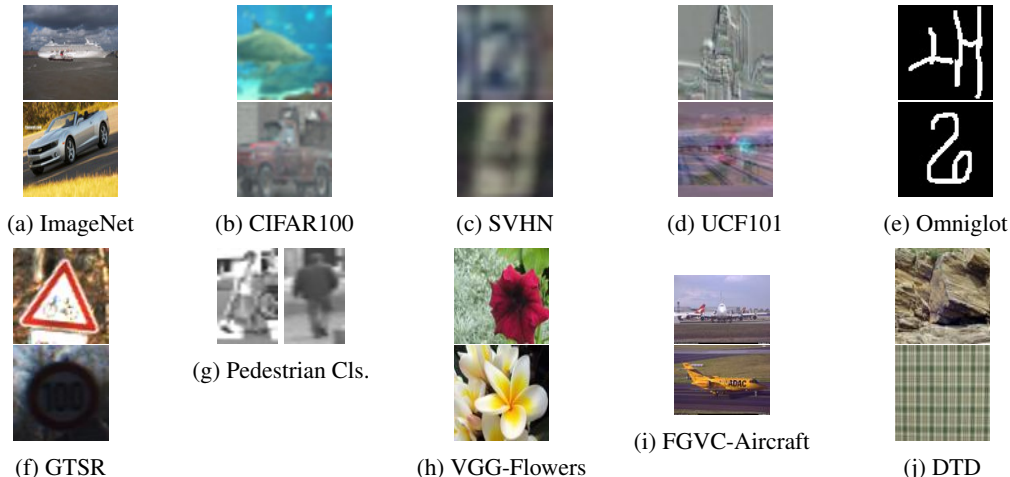


Figure 6: Example images from the VDD benchmark (Rebuffi et al., 2017a). Each task has a significantly different domain than others, making VDD a challenging benchmark for lifelong learning.

- *Preliminary Results on Class-Incremental Settings:* We show that the task similarity used in our sampling may have the potential of developing class-incremental lifelong learning in Sec. K.

B DATASET DETAILS

B.1 THE VDD BENCHMARK

It consists of 10 tasks: ImageNet12 (Russakovsky et al., 2015), CIFAR100 (Krizhevsky et al., 2009), SVHN (Netzer et al., 2011), UCF101 Dynamic Images (UCF) (Soomro et al., 2012; Bilen et al., 2016), Omniglot (Lake et al., 2015), German Traffic Signs (GTSR) (Stallkamp et al., 2012), Daimler Pedestrian Classification (DPed) (Munder & Gavrila, 2006), VGG Flowers (Nilsback & Zisserman, 2008), FGVC-Aircraft (Maji et al., 2013), and Describable Textures (DTD) (Cimpoi et al., 2014). All the images in the VDD benchmark have been scaled such that the shorter side is 72 pixels. Table 6 shows the number of samples in each task. Figure 6 shows examples of images from each task of the VDD benchmark.

In our experiments, we use 10% of the official training data from each of the tasks for validation (e.g., used in the target network selection in Section 3.2.3), and report the accuracy on the official validation set for fair comparison with the learn-to-grow method (Li et al., 2019) in Table 8. In Table 6, the train, validation and test splits are thus referred to 90% of the official training data, 10% of the official training data, and the entire official validation data respectively. When finetuning the learned architecture, we use the entire the official training data to train and report results on the the official validation set.



Figure 7: Example images from the 5-Datasets benchmark (Ebrahimi et al., 2020).

B.2 THE 5-DATASETS BENCHMARK

It consists of 5 tasks: CIFAR10 (Krizhevsky et al., 2009), MNIST (Lecun et al., 1998), Fashion-MNIST (Xiao et al., 2017), not-MNIST (Bulatov, 2011), and SVHN (Netzer et al., 2011). Table 7 shows the data statistics. Figure 7 shows examples of images from each task. To be consistent with the settings used on the VDD benchmark, we use

15% of the training data for validation and report the results on the official test data, except for not-MNIST for which an official test split is not available. So, for the not-MNIST dataset, we use the small version of that dataset, with which we construct the test set by randomly sampling 20% of the samples. From the remaining 80%, we use 15% for validation, and the rest as the training set.

Task	Train	Validation	Test
ImageNet12	1108951	123216	49000
CIFAR100	36000	4000	10000
SVHN	42496	4721	26040
UCF	6827	758	1952
Omniglot	16068	1785	6492
GTSR	28231	3136	7842
DPed	21168	2352	5880
VGG-Flowers	918	102	1020
Aircraft	3001	333	3333
DTD	1692	188	1880

Table 6: The number of samples in training, validation and testing sets per task used in our experiments on the VDD benchmark (Rebuffi et al., 2017a).

Task	Train	Validation	Test
MNIST	51000	9000	10000
not-MNIST	12733	2247	3744
SVHN	62269	10988	26032
CIFAR10	42500	7500	10000
Fashion MNIST	51000	9000	10000

Table 7: Number of samples in training, validation, and test sets per task in the 5-Datasets benchmark (Ebrahimi et al., 2020). The test samples have been reported from the official test data provided by each individual dataset, except for not-MNIST. See text for details.

C THE VISION TRANSFORMER: ViT-B/8

We use the base Vision Transformer (ViT) model, with a patch size of 8×8 (ViT-B/8) model from (Dosovitskiy et al., 2021). The base ViT model which contains 12 Transformer blocks with residual connections for each block. A Transformer block is defined by stacking a Multi-Head Self-Attention (MHSA) block and a Multi-Layer Perceptron (MLP) block with residual connections for each block. ViT-B/8 uses 12 attention heads in each of the MHSA blocks, and a feature dimension of 768. The MLP block expands the dimension size to 3072 in the first layer and projects it back to 768 in the second layer. For all the experiments, we use an image size of 72×72 following the VDD setting. We base the implementation of the ViT on the `timm` (Wightman, 2019) package.

D IMAGENET TRAINING

To train the ViT-B/8 model, we use the ImageNet data provided by the VDD benchmark (the `train` split in Table 6). To save the training time, we initialize the weights from the ViT-B/8 trained on the full resolution ImageNet dataset (224×224) and available in the `timm` package, and finetune it for 30 epochs on the downsized version of ImageNet (72×72) in the VDD benchmark. We use a batch size of 2048 split across 4 Nvidia Quadro RTX 8000 GPUs. We follow the standard training/finetuning recipes for ViT models. The file `artihippo/logs/imagenet_pretraining/args.yaml` provides all the training hyperparameters used for training the the ViT-B/8 model on ImageNet. During testing, we take a single center crop of 72×72 from an image scaled with the shortest side to scaled to 72 pixels.

E BACKGROUND ON THE LEARN-TO-GROW METHOD

The learn-to-grow method (Li et al., 2019) uses Differentiable Architecture Search (DARTS) (Liu et al., 2019a), a supernet based NAS algorithm to learn a strategy for reusing, adapting, or renewing the parameters learned for the previous tasks (skipping is not applied). Consider an L -layer backbone network with \mathcal{S}^l choice of parameters for a layer l learned for the previous tasks. The parameters can be the weights and biases of the layer in the case of fully-connected layers, or the filters and the biases in the case of a Convolutional layers. For a new task, the learn-to-grow method constructs the search space for NAS (referred to as operations) by applying the operation operations `reuse`, `adapt`, and `new` to \mathcal{S}^l for all layers $l \in [1, L]$. The total number of choices for layer l is $C_l = 2|\mathcal{S}^l| + 1 \{|\mathcal{S}^l| \text{ reuse}, |\mathcal{S}^l| \text{ adapt, and } 1 \text{ new operation}\}$. Following DARTS, the output of a layer when training the NAS supernet is given by

$$x_{out}^l = \sum_{c=1}^{C_l} \frac{\exp(\alpha_c^l)}{\sum_{c'=1}^{C_l} \exp(\alpha_{c'}^l)} g_c^l(x_{in}^l), \quad (7)$$

where $g_c^l(\cdot)$ is defined by,

$$g_c^l(x_{l-1}) = \begin{cases} S_c^l(x_{in}^l) & \text{if } c \leq |\mathcal{S}^l|, \\ S_c^l(x_{in}^l) + \gamma_{c-|\mathcal{S}^l|}^l(x_{in}^l) & \text{if } |\mathcal{S}^l| < c \leq 2|\mathcal{S}^l|, \\ \text{new}^l(x_{in}^l) & \text{if } c = 2|\mathcal{S}^l| + 1, \end{cases} \quad (8)$$

where γ denotes the additional operation used in parallel (1×1 convolution in the case of a Convolutional layer) which implements the `adapt` operation. Using DARTS, the operations are trained jointly with architecture coefficients α_c^l . Once the supernet is trained, the optimal operation is selected such that $(c^*)^l \leftarrow \text{argmax}_c \alpha_c^l$. In experiments, the learn-to-grow method uses a 26-layer ResNet (He et al., 2016) on the VDD benchmark.

Remarks on the proposed learning-to-grow with ViTs. The learn-to-grow method (Li et al., 2019) can maintain dynamic feature backbone networks for different tasks based on NAS, which leads to the desired selectivity and plasticity of networks in lifelong learning. It has been mainly studied with Convolutional Neural Networks (CNNs), and often apply DARTS for all layers with respect to the three operations, which is time consuming and may be less effective when a new task has little data.

More importantly, the vanilla learn-to-grow method with DARTS and ResNets does not have the motivation of integrating learning and (long-term) memory in lifelong learning, which is the focus of our proposed ArtiHippo method. In learning a new task, unlike the vanilla learn-to-grow method in which all the previous tasks are treated equally when selecting the operation operations, our proposed ArtiHippo leverages the task similarities which in turn exploits the class-token specialized in ViTs.

F COMPARISON WITH LEARN TO GROW (LI ET AL., 2019)

For completeness, we Table 2 with the results reported on the VDD benchmark by Learn to Grow (Li et al., 2019). Although not directly comparable, our method does show consistent performance trend across tasks, compared with the ResNet-based (He et al., 2016) DARTS-optimized (Liu et al., 2019a).

Model	NAS	Method	ImNet	C100	SVHN	UCF	OGIt	GTSR	DPed	Flwr	Airc.	DTD	Avg. Accuracy
ResNet	-	Adapter	69.84	79.82	94.21	70.72	85.1	99.89	99.58	60.29	50.11	50.60	76.02
	DARTS	L2G	69.84	79.59	95.28	72.03	86.6	99.72	99.52	71.27	53.01	49.89	77.68
ViT-B/8 (#Params: 86.04M, FLOPs: 7.11G)	-	S-Prompts [†] (p=1/task)	82.65	86.69	69.89	51.95	49.55	94.07	99.25	90.39	35.03	56.19	71.57 ± 0.31
	-	L2P [†] (p=12/task)	82.65	89.06	81.43	63.99	62.86	98.21	99.77	94.58	45.00	60.78	77.83 ± 0.28
FLOPs: 7.11G)	SPOS + Hierarchical Sampling	ArtiHippo	82.65	85.50	95.63	74.09	82.53	99.93	99.85	79.31	41.62	41.21	78.23 ± 0.93
		ArtiHippo	82.65	90.92	95.93	77.08	84.14	99.92	99.80	77.76	47.11	45.79	80.11 ± 1.17
		ArtiHippo (p=1/task)	82.65	90.99	95.87	78.98	86.12	99.91	99.89	88.20	45.86	51.31	81.98 ± 0.95

Table 8: Results on the VDD benchmark (Rebuffi et al., 2017a). The results on L2G and Adapter are adopted from the L2G paper (Li et al., 2019). The task order is based on the one used in the L2G method. Our method shows clear improvements over the previous approaches. The proposed hierarchical sampling performs better than uniform sampling. All the results from our experiments are averaged over 3 different seeds.

G BACKGROUND ON THE SINGLE-PATH ONE-SHOT NEURAL ARCHITECTURE SEARCH METHOD

DARTS (Liu et al., 2019a) trains the entire supernet jointly in learning a new task, and thus might not be practically scalable and sustainable after the supernet “grew too fat” at each layer. The strategy used in Single-Path One-Shot (SPOS) (Guo et al., 2020) NAS offers an alternative strategy based on a *stochastic* supernet. It uses a bi-level optimization formulation consisting of the supernet training and the target network selection,

$$W_{\mathcal{A}} = \text{argmin}_W \mathcal{L}_{train}(\mathcal{N}(\mathcal{A}, W)), \quad (9)$$

$$a^* = \text{argmax}_{a \in \mathcal{A}} \text{Acc}_{val}(\mathcal{N}(a, W_{\mathcal{A}}(a))), \quad (10)$$

where Eqn. 9 is solved by defining a prior distribution $\Gamma(\mathcal{A})$ over the choice of operations in the stochastic supernet and optimizing,

$$W_{\mathcal{A}} = \text{argmin}_W \mathbf{E}_{a \sim \Gamma(\mathcal{A})} \mathcal{L}_{train}(\mathcal{N}(\mathcal{A}, W)). \quad (11)$$

This amounts to sampling one operation per layer (i.e., one-shot) of the neural network, and to forming a single path in the stochastic supernet. Eqn. 10 is optimized using an evolutionary search based on the validation performance for different candidates of the target network in a population, which is efficient since only inference is executed. The SPOS method empirically finds that a uniform prior works well in practice, especially when sufficient exploration is afforded. Note that this prior is also applied in generating the initial population for the evolutionary search.

The evolutionary search method used in the SPOS method is adopted from (Real et al., 2019). It first initializes a population with a predefined number of candidate architectures sampled from the supernet. It then “evolves” the population via the crossover and the mutation operations. At each “evolving” iteration, the population is evaluated and sorted based on the validation performance. With the top- k candidates after evaluation and sorting (the number k is predefined), for crossover, two randomly sampled candidate networks in the top- k are crossed to produce a new target network. For mutation, a randomly selected candidate in the top- k mutates its every choice block with probability (e.g., 0.1) to produce a new candidate. Crossover and mutation are repeated to generate sufficient new candidate target networks to form the population for the next “evolving” iteration.

Remarks on the proposed hierarchical task-similarity-oriented sampling with exploration-exploitation trade-off. We modify the core sampling component in the SPOS algorithm for resilient lifelong learning with a long-term memory. During exploitation, we generate the prior $\Gamma(\mathcal{A})$ using our proposed hierarchical sampling scheme, and use the uniform prior during exploration. The same sampling scheme is applied when generating the initial population for the evolutionary search as well.

H MODIFYING S-PROMPTS AND L2P FOR TASK-INCREMENTAL SETTING

Both, Learn to Prompt and S-Prompts, can be modified for task-incremental setting without altering the core algorithm for learning the prompts. For S-Prompts, this is done by training a separate task token (i.e. a `cls` token) per task and retrieving the correct token using the task ID. For L2P, we follow the official implementation¹ used for evaluating on the 5-datasets benchmark. L2P first trains a set of N prompts of length L_p (i.e. NL_p tokens) per task. It then learns a set of N keys such that the distance between the keys and the image encoding (using a fixed feature extractor) is maximized. We retrieve the correct prompts using the Task ID instead of using a key-value matching and make L2P compatible with a task-incremental setting. We initialize the values for the prompts for task t from the trained values of task $t - 1$ following the original implementation.

I SETTINGS AND HYPERPARAMETERS IN THE PROPOSED LIFELONG LEARNING

Starting with the ImageNet pretrained ViT-B/8, the proposed lifelong learning methods consists of three components in learning new tasks continually and sequentially: supernet training, evolutionary search for target network selection, and target network finetuning. The supernet training and target network finetuning use the `train` split, while the evolutionary search uses the `validation` split, both shown in Table 6 and Table 7. We use the vanilla data augmentation in both supernet training and target network finetuning.

Data Augmentations. A full list of data augmentations used for the VDD benchmark is provided in Table 9, and the data augmentations used for the tasks in the 5-datasets benchmark is provided in Table 10. The augmentations are chosen so as not to affect the nature of the data. Scale and Crop transformation scales the image randomly between 90% to 100% of the original resolution and takes a random crop with an aspect ratio sampled from a uniform distribution over the original aspect ratio ± 0.05 . In evaluating the supernet and the finetuned model on the validation set and test set respectively, images are simply resized to 72×72 with bicubic interpolation.

Task	Scale and Crop	Hor. Flip	Ver. Flip
CIFAR100	Yes	p=0.5	No
Aircraft	Yes	p=0.5	No
DPed	Yes	p=0.5	No
DTD	Yes	p=0.5	p=0.5
GTSR	Yes	p=0.5	No
OGIt	Yes	No	No
SVHN	Yes	No	No
UCF101	Yes	p=0.5	No
Flwr.	Yes	p=0.5	No

Table 9: Data augmentations for the 9 tasks in the VDD benchmark.

Task	Scale and Crop	Hor. Flip
MNIST	Yes	No
not-MNIST	Yes	No
SVHN	Yes	No
CIFAR100	Yes	p=0.5
Fashion MNIST	Yes	No

Table 10: Data augmentations used for each task in the 5-Datasets benchmark.

¹L2P official implementation: <https://github.com/google-research/l2p>

I.1 SUPERNET TRAINING

VDD Benchmark: For each task, we train the supernet for 300 epochs. We use a label smoothing of 0.1. No other form of regularization is used since the `skip` operation provides implicit regularization, which plays the role of Drop Path during training. We use a learning rate of 0.001 and the Adam optimizer (Kingma & Ba, 2014) with a Cosine Decay Rule. For experiments with separate class tokens per task, we use a learning rate of 0.0005 for training the supernet, and 0.003 for training the task token. For each epoch, a minimum of 15 batches are drawn, with a batch size of 512. If the number of samples present in the task allows, we draw the maximum possible number of batches that covers the entire training data.

5-datasets Benchmark: We use the same hyperparameters as those used in the VDD Benchmark, but train the supernet for 150 epochs.

I.2 EVOLUTIONARY SEARCH

The evolutionary search is run for 20 epochs. We use a population size of 50 and a mutation probability of 0.1. 25 candidates are generated by mutation, and 25 candidates are generated using crossover. The top 50 candidates are retained. The crossover is performed among the top 10 candidates.

I.3 FINETUNING

The target network for a task selected by the evolutionary search is finetuned for 30 epochs with a learning rate of 0.001, Adam optimizer, and a Cosine Learning Rate scheduler. Drop Path of 0.25 and label smoothing of 0.1 is used for regularization. We use a batch size of 512, and a minimum of 30 batches are drawn. When using a separate task token for each task, the task token is first finetuned with a learning rate of 0.001.

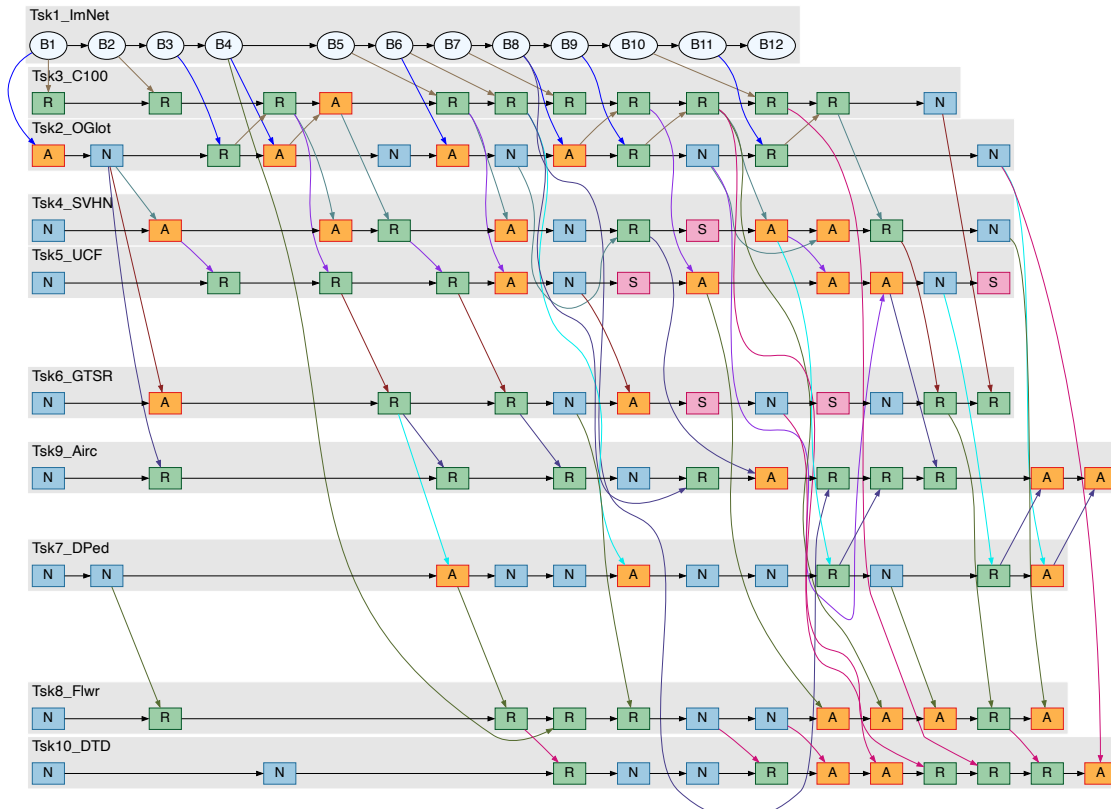


Figure 8: Architecture learned for task sequence ImNet, OGI, C100, SVHN, UCF, GTSR, DPed, Flwr, Airc, DTD

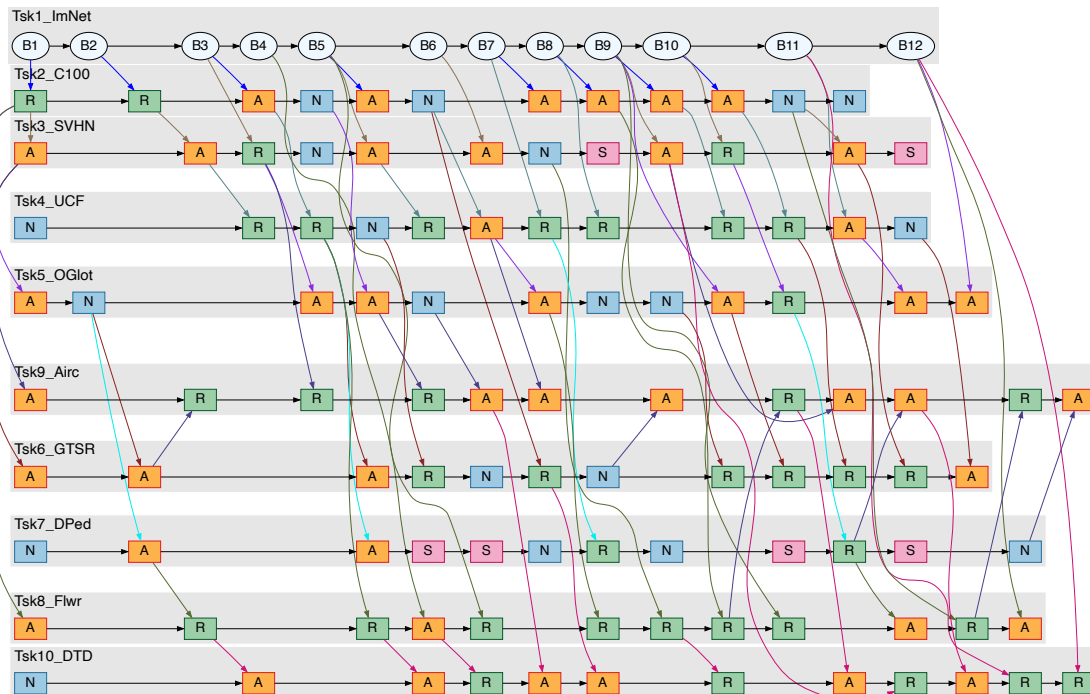


Figure 9: Architecture learned using pure exploration. Pure Exploration based method adds many unnecessary Adapt and New operations even though the tasks are similar (ImNet \rightarrow C100), proving the effectiveness of the proposed sampling method

I.4 NORMALIZED COSINE SIMILARITY

To verify the use of the Normalized Cosine Similarity as our similarity measure (Eqn. 6 in the main text), we refer to Figure 10. Figure 10a shows the Cosine Similarity between the mean class-tokens learned for tasks ImageNet, CIFAR100, SVHN, and UCF101 (in order), and the mean class-tokens calculated for each expert using the data from the current task Omniglot. Empirically, we observe that the Cosine Similarity between the mean class-tokens calculated using the data of the task associated with an expert and the mean class-token calculated with the current task in training is high. However, the difference between the similarity values for each expert are more important than the absolute values of the similarity. This difference can be increased by scaling the similarity such that it increases the magnitude difference between the similarities of different tasks, but maintains the relative similarity. This can be achieved by scaling the Cosine Similarities between -1 and 1 using the minimum and the maximum values from all the experts and all the blocks (Figure 10b). Using the Normalized Cosine Similarity leads to better and more intuitive probability distributions for sampling candidate experts and the retention probabilities for the sampled experts. For example, comparing the probability values for sampling an expert at Block 6 calculated using Cosine Similarity (Figure 10c) vs. Normalized Cosine Similarity (Figure 10d), the probability of sampling the ImageNet expert increases, and those of sampling UCF101 and Omniglot decrease. Similarly, for Blocks 3, 4 and 5, the retention probability calculated using the Normalized Cosine Similarity (Figure 10f) reduces by a large factor than that calculated using the Cosine Similarity (Figure 10e). This will encourage sampling the new and the skip experts.

J LEARNED ARCHITECTURE FOR DIFFERENT TASK ORDER AND PURE EXPLORATION

Figure 8 shows the architecture learned for a different task sequence. It can be seen that even with a different task sequence, the proposed method can learn to exploit task similarities. For example, a new projection layer is learned in Block 2 for Omniglot, which is adapted by SVHN and GTSRB. Figure 9 shows the architecture learned using a pure exploration strategy. It can be seen that pure exploration does not reuse components from similar tasks. For example, a large number of Adapt and New are added when learning CIFAR100. In contrast, the exploitation-exploitation strategy can learn to reuse the components from the ImageNet task (Figure 4), and achieves better accuracy as well (Table 2).

Method	Average Accuracy	
	5-Datasets	VDD
Max	34.35 ± 15.75	32.96 ± 2.07
Minimum Entropy	66.09 ± 3.98	45.69 ± 1.96

Table 11: Average Accuracy in a class-incremental setting using the proposed methods. The results for 5-datasets benchmark have been averaged over 5 different task orders, whereas the results on the VDD benchmark have been averaged over the same tasksequence but different random seeds.

K PRELIMINARY RESULTS ON EXTENDING THE ARTIHIPPO FOR CLASS-INCREMENTAL SETTINGS

The similarity based sampling method can be naturally extended to a class-incremental setting where the task indices are not available at test time. We calculate the similarity between the class token at each block of the ViT when performing predictions with an image. This is done for each task by activating the correct set of experts associated with the task. For each task, this generates L similarity scores, where L is the number of blocks in the transformer

$$S_t^l = \text{CosineSim}(\mu_{e_t}, x_0^l) \quad (12)$$

where x_0^l is the class token at block l . Note that we do not normalize the cosine similarity. The similarity scores for all the blocks are combined to form an indicator score $I^t(x)$ per task. The test image is assigned the index of the task with the highest indicator score: $t \leftarrow \text{argmax}_t I^t(x)$.

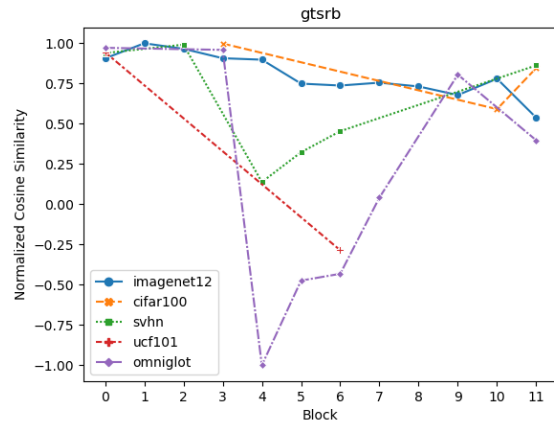
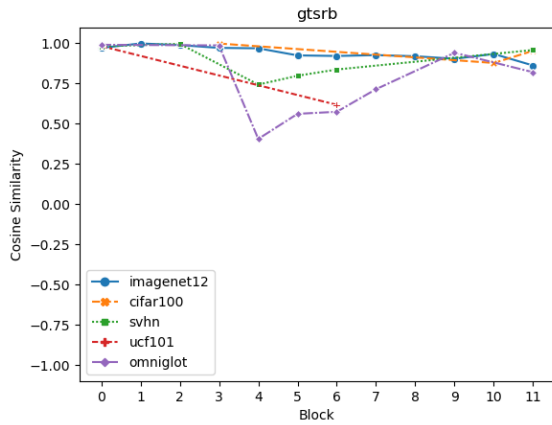
We explore two methods:

Max: For each task, the maximum similarity score from all the blocks is chosen as the indicator score

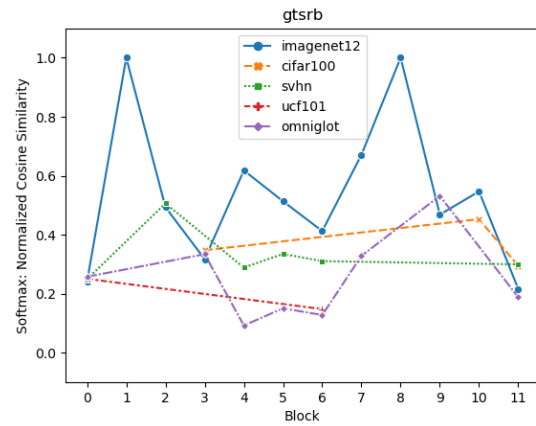
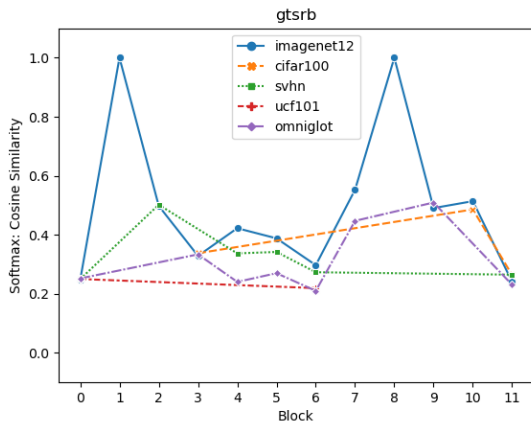
$$I^t(x) = \max(S_{1:L}^t)$$

Minimum Entropy: For each task, the entropy using each path is calculated, and the task for which the classification head shows the minimum entropy is chosen.

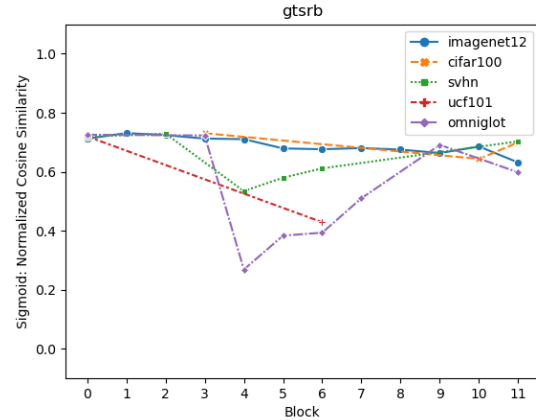
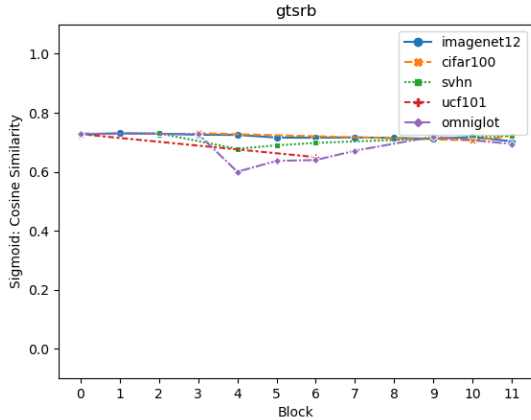
Table 11 shows the average accuracies obtained on the 5-datasets benchmark. The low accuracy scores suggest that although the mean class token is suitable for sampling in the supernet training and the evolutionary search, its applicability is limited for task agnostic inference. However, the results are promising, and could be made better by introducing a mixture of class-tokens per task to account for the variations in tasks, similar in spirit to the mixture modeling of experts of ArtiHippo and the learn-to-prompt method (Wang et al., 2022c), which we leave for future work.



(a) Cosine Similarity between the mean class-tokens from the (b) Normalized Cosine Similarity at each block calculated by



(c) Probabilities of sampling candidate Expert $e(\psi_e^l)$ at each (d) Probabilities of sampling candidate Expert $e(\psi_e^l)$ at each



(e) Retention probabilities (ρ_e^l) for each expert in each block, calculated using the Cosine Similarity. (f) Retention probabilities (ρ_e^l) for each expert in each block, calculated using the Normalized Cosine Similarity.

Figure 10: Comparison of probability values for sampling the Experts (Middle row) and the retention probabilities (Bottom row) using the Cosine Similarity and the Normalized Cosine Similarity. Using the Normalized Cosine Similarity gives better probability values for ψ_e , as can be seen in Block 6. Using Normalized Cosine Similarity increases the probability of sampling the SVHN expert. The effect on the retention probability ρ_e can be prominently seen on the Omniglot experts. The retention probability in Blocks 4 to 6 **10f** reduces below 0.5, which will encourage the new and skip experts to be trained and selected in the evolutionary search even if Omniglot experts were sampled.